Resource Accumulation, Conflict, and the Development of Africa*

Achyuta Adhvaryu†
James Fenske‡
Gaurav Khanna§
Anant Nyshadham¶

Preliminary draft, May 15, 2015. Methods and results may change.

Abstract

African development is tied to the frequency and intensity of conflict. Growth and conflict, in turn, are simultaneously driven by the accumulation and distribution of resources. To characterize these linkages, we develop a simple model of resource accumulation and conflict between neighboring societies. Resources fuel conflict through a rapacity effect; that is, by raising the gains from appropriation. Resources also encourage conflict through an endowment effect that increases fighting strength. Both absolute and relative levels of resources available to each party matter for conflict. The relationship between income and development is non-monotonic, determined directly by resource accumulation but also by the incidence of conflict. We test the model using spatial data on long-run rainfall patterns, conflict, and nighttime lights, and find strong evidence in favor of its predictions. We find similar results using alternative measures of resource accumulation, including land productivity, oil fields, and minerals. These results are not driven by local geographic, agricultural, or climatological differences, and are robust to tight spatial fixed effects.

Keywords: Conflict, Resource Curse, Development, Africa JEL Classification Codes: D74, O10, O40, N17, N47

*Adhvaryu gratefully acknowledges funding from the NIH/NICHD (5K01HD071949).
†University of Michigan, adhvaryu@umich.edu, achadhvaryu.com
‡University of Oxford, james.fenske@economics.ox.ac.uk, jamesfenske.com
§University of Michigan, gkhanna@umich.edu, gauravkhanna.info
¶University of Southern California, nyshadha@usc.edu, anantnyshadham.com

1 Introduction

Conflict frequently interrupts African economic development (Besley and Persson, 2011). The accumulation of resources is disrupted by conflict through several channels, including the destruction of lives and capital, reduced investment, and trade diversion (Abadie and Gardeazabal, 2003; Blattman and Miguel, 2010; Glick and Taylor, 2009). The resource accumulation that fuels economic growth also spurs conflict, as the gains from appropriation rise (Caselli et al., 2013; Dube and Vargas, 2013; Fearon, 2005). Where this appropriation motive is strong, resource windfalls may actually hamper development (Bannon and Collier, 2003; Sachs and Warner, 1995). Further, additional resources can empower the state and its rivals and so may be used to fuel destructive activities or repression (Acemoglu and Robinson, 2001; Caselli and Tesei, 2011; Nunn and Qian, 2014).

The patterns over space that correlate conflict prevalence and development with historical rainfall are consistent with the mechanisms highlighted in earlier studies. In Figure 1, we proxy for development by plotting log light density against rainfall over the past 10 years for 0.5° by 0.5° grid cells across Africa, grouped into bins. The resulting association is clearly non-monotonic: areas with the greatest historical rainfall accumulation are no more developed than countries with very low levels of rainfall. Figure 2 may help explain this inverse U-shape. In it, we graph conflict incidence against historical rainfall for African countries in the same time period. The result is different from Figure 1: conflict is positively associated with historical rainfall, with a convex trend for areas with the highest levels of rainfall accumulation. Though certainly not conclusive, these associations offer some preliminary evidence of the potentially perverse effects of resource accumulation on economic development through heightened conflict risk.

In this paper, we study the linkages between resources, the incidence of conflict, and economic development. We develop a simple model in which two groups decide simultaneously whether or not to engage in conflict. Offensive and defensive capacities for each group increase with accumulated resources. This endowment effect of resources on conflict is a feature of early models of conflict in the state of nature (e.g. Grossman and Kim (1995); Hirshleifer (1989)) though it has not featured prominently in recent empirical or theoretical work. We capture a rapacity effect by positing that each group's return to fighting is increasing in the neighboring group's resources. There is a fixed cost of participating in conflict. If both groups choose not to fight, the result is peace. If one group chooses to fight but the other does not, the former succeeds at appropriating a fraction of the latter's resources with probability 1. If both groups fight, the probability of success is

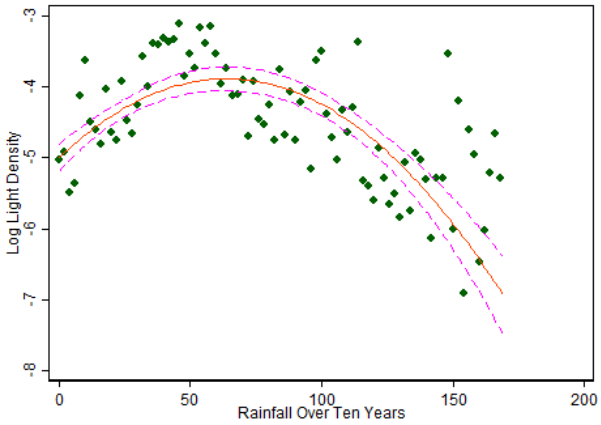

Figure 1: Log Light Density vs. Rainfall over the past ten years

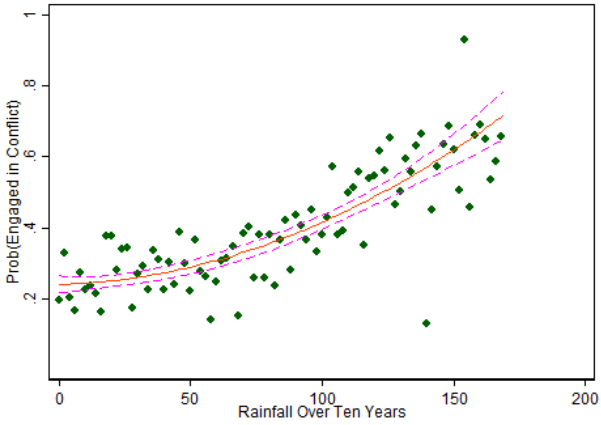

Figure 2: Being Engaged in a Conflict vs. Rainfall

Observations for 0.5° by 0.5° grid cells across Africa. Graphs plot quadratic fits with confidence intervals of the relationship between annual rainfall (in mm) averaged over a ten period (1998-2008) against (1) Log (Light Density) in 2008 and (2) Whether the region was engaged in conflict between 1998 and 2008. Binned means in scatter plots are binned at the 2mm rainfall level.

determined by the relative strength of each group, which itself depends on endowments.

Nash equilibria in this model are determined by the resource endowments of each group (along with other fundamentals such as the cost of raiding and the fraction appropriated when raiding successfully). When both groups have low levels of resource accumulation, peace results. This is because neither group has much strength, and the gains from raiding are also not high for either group, since the contestable resources are few. When one group has accumulated *slightly more* resources (loosely speaking) than the other, a one-sided conflict equilibrium results, in which the relatively resource-poor group raids while the other chooses not to retaliate. When both groups have abundant resources, both are impelled to war.

In our baseline model, the only way in which the two groups interact is through the potential conflict between them. We extend the model by incorporating a sharing rule, and show within this augmented framework that societies who share more (e.g., who are spatially close, residing in the same country or agro-ecological zone, or from areas dominated historically by the same ethnic group) are less likely to choose war.

We test the model's predictions using disaggregated spatial data on long-run rainfall patterns, conflict, and satellite data on nighttime lights. We partition the African continent

into a 0.5 x 0.5 degree grid. At each point, we match the 10-year historical average of rainfall (from 1998 to 2008) to the number of conflict events and the intensity of nighttime lights at that point. We then match these points (i) to all their neighbors (j) within a 500 kilometer radius. Using conflict data from the Peace Research Institute Oslo (PRIO), we ascertain for each ij whether this *pair* was involved in shared conflict over the past 10 years. We also measure the distance between i and j, and a variety of characteristics of the two points (e.g., geographic variables, country, historically predominant ethnic group).

As summarized above, the model's main implications concern the partitioning of the ij "resource space" into Nash equilibria regions. In the empirical analysis below, we begin by drawing contour plots of the raw data on i and j historical rainfall on the x and y axes, and involvement of i and j in shared conflict on the z axis. In these simple plots, we find striking confirmation of the model's main implications regarding equilibria regions over the ij resource space. Groups represented by our disaggregated points i and j behave in a manner entirely consistent with the predictions of our simple static model in the cross section.

Throughout the analysis we will be focusing on the longer-run accumulation of resources rather than contemporaneous shocks. In the immediate aftermath of a shock, there is often a greater likelihood of conflict because of the reduced opportunity cost of going to war (Grossman, 1991). This pattern, where better resource shocks lower the likelihood of war, has been well established in the empirical literature (Brückner and Ciccone, 2010; Hsiang et al., 2013; Jia, 2014; Miguel and Satyanath, 2011). Over the longer-run, however, we may expect different outcomes. Greater resource accumulation can lead to a larger pie to fight over, leading to a 'rapacity effect (Grossman, 1991; Hirshleifer, 1989; Skaperdas, 1992). Furthermore, better access to resources allows parties to raise stronger militia or build state-capacity for counter-insurgencies (Bazzi and Blattman, 2014; Besley and Persson, 2010). The longer-run accumulation of wealth could make one party relatively stronger and more likely to succeed in appropriating its rival's resources, and so could increase the likelihood of conflict.

The literature has distinguished between the opportunity-cost effect and the 'rapacity effect' by studying the type of shocks, who owns the resources, and the location and type of resource (Berman et al., 2014; Caselli et al., 2013; Dube and Vargas, 2013). Similarly, different resources may accumulate over different spans of time. Wages may fall in the immediate aftermath of a negative shock, and lower the opportunity cost of war. Alternatively, building armies and accumulating appropriable wealth is a longer procedure,

during which the state-capacity effect or the rapacity effect may be more relevant.

Our formal test of these implications involves finding a (two-dimensional) structural break in the relationship between i and j historical rainfall on the one hand and conflict between the two groups on the other. Our empirical approach is an extension of structural break methods used by Card et al. (2008) and Gonzalo and Wolf (2005), in which we use two-thirds of the sample to find the optimal cutoff and the remaining one-third to do regression analysis using the estimated cutoff value. We cluster standard errors using conservatively defined geographic levels to account for potential spatial correlation in the error term.

Our results using the structural break method outlined above, as well as controlling for local geographic, agricultural, climatological characteristics, and spatial fixed effects, generates evidence in line with the contour plot evidence and in strong support of the model's predictions. We supplement this evidence with optimal bandwidth regression discontinuity (RD) results (Calonico et al., 2014) at the estimated cutoffs, which show that conflict rises discontinuously when crossing the threshold from a peace to a conflict equilibrium region.

Finally, we draw similar contour plots for satellite data on nighttime lights, to highlight how the resource accumulation-conflict dependency results in a complex reduced form relationship between resource abundance and development. Again, we find striking confirmation of the model's predictions in these contour plots of light intensity. RD evidence supports this story, showing that moving across the optimally determined threshold into a conflict-prone Nash region of the resource space generates a fall in nighttime lights despite being at a higher level of resource accumulation.

Our study relates to three main strands of work in economics. First, we contribute to the literature on the causes of conflict. A growing body of work demonstrates the causal impacts of a wide variety of drivers – population, weather, natural resources, other forms of income, history, culture, and institutions – on the incidence of conflict. This literature puts particular focus on Africa, given that continent's particularly long and intense history of conflict.[1] We add to this literature by studying a more disaggregated level than countries, by emphasizing the accumulation of resources over the medium to long term, and by focusing on perhaps the most common method of income accumulation

[1]See, for example, Arbatli et al. (2015); Berman and Couttenier (2014); Brückner (2010); Caselli et al. (2013); Caselli and Tesei (2011); Esteban et al. (2010); Michalopoulos and Papaioannou (2011); Rohner et al. (2013).

in Africa to date – rain-fed agriculture.

Second, we add to the literature on the role of geographic endowments in development. Geography and its correlates matter, particularly in Africa (Acemoglu et al., 2001; Alexeev and Conrad, 2009; Alsan et al., 2013; Barrios et al., 2010; Dell et al., 2012; Mehlum et al., 2006; Nunn and Puga, 2012). Rather than focusing on the immediate effects of endowment shocks, we study the accumulation of resources over a longer period of time. Furthermore, this literature does not give substantial focus to spatial externalities: how does one group's resource accumulation help or hurt a neighbor's development? We point to conflict as a primary mechanism for this externality. By examining both conflict and luminosity, our study looks at these mechanisms as well as the ultimate effects on development.

Third, we study strategic interactions between rival factions in the face of economic shocks (Mitra and Ray, 2013). While most of the conflict literature focuses on shocks to one of the parties concerned, it is crucial to understand how shocks to a rival group can affect one's own likelihood of engaging in conflict. Given that this interaction is strategic, a game-theoretic model is necessary to outline the conditions that may lead to the outbreak of conflict. Such strategic complementarities featured in the early literature on conflict (Grossman, 1991), but have largely been overlooked in recent empirical work.

The remainder of the paper is structured as follows. Section 2 sets up our model and delivers its main predictions through a set of lemmas and propositions. Section 3 describes our data. Section 4 details our empirical strategy, and section 5 describes our results. Finally, section 6 is a concluding discussion.

2 Model

We model the interaction of two parties, i and j, who play a simultaneous game that determines peace or conflict between them. The parties choose strategies s from the set $\{R, N\}$, where R denotes the decision to raid (i.e., engage in conflict), and N denotes the decision not to raid. We denote a strategy profile by (s_i, s_j) for $s_i, s_j \in \{R, N\}$.

Each party is endowed with wealth, denoted $r_i, r_j \in (0, \infty)$ for resources in i and j, respectively. If neither party raids ((N, N)), each keeps its own wealth. If a party raids, it expends fixed cost c in conflict, which we assume for simplicity is the same for i and j. If

a party raids *successfully*, it seizes a fraction δ of the opposing party's wealth. If one party raids and the other chooses not to fight ((R, N) or (N, R)), the raiding party succeeds with probability 1. If, on the other hand, both parties choose to raid ((R, R)), then success for i occurs with probability $p := \frac{r_i}{r_i + r_j}$.[2] If i wins in this scenario, it seizes a proportion δ of j's *remaining* assets, i.e. $\delta(r_j - c)$.

The game is summarized in Figure 3. Note that in (R, R), we evaluate the expected payoff to each party given probability of success p defined above.

2.1 Best Responses

The best responses of each player to the other's actions depend on the model parameters, and in particular the realizations of wealth r_i and r_j. The following lemma determines the best response functions (denoted $BR_k(s_{-k})$ for $k \in \{i, j\}$) for i and j with wealth $(r_i, r_j) \in \mathbb{R}^2_+$.

Proposition 2.1 *The following are best response functions for agent k:*

1. $BR_k(s_{-k} = N) = \begin{cases} R, & \text{if } r_{-k} > \frac{c}{\delta} \\ N, & \text{else} \end{cases}$
2. *Let* $\psi(r_k) := \frac{-\delta r_k^2 + c(1+\delta) r_k}{\delta r_k - c(1-\delta)}$.

   $BR_k(s_{-k} = R) = R$, *for all* (r_k, r_{-k}) *such that*

$$\{(r_k, r_{-k}) : r_k \in (c\frac{1-\delta}{\delta}, \infty), r_{-k} > \psi(r_k)\} \tag{1}$$

   And $BR_k(s_{-k} = R) = N$, *for all* (r_k, r_{-k}) *such that*

$$\{(r_k, r_{-k}) : r_k \in (0, c\frac{1-\delta}{\delta})\} \cup \{(r_k, r_{-k}) : r_k \in (c\frac{1-\delta}{\delta}, \infty), r_{-k} < \psi(r_k)\} \tag{2}$$

[2] We choose this functional form for p for its parsimony and because intuitively p should be increasing in r_i and decreasing in r_j.

2.2 Equilibria

These best response functions help characterize the set of pure strategy Nash Equilibria in the (r_i, r_j) space. Figure 4 divides the (r_i, r_j) space into the Nash Equilibrium regions. The space can then be described by the following lemmas which are proved in Appendix A.1.:

1. For $r_i, r_j \in (0, \frac{c}{\delta})$, (N, N) is the unique pure-strategy Nash Equilibrium.
2. Let $\psi(r_k) := \frac{-\delta r_k^2 + c(1+\delta) r_k}{\delta r_k - c(1-\delta)}$. (R, R) is the unique pure strategies Nash Equilibrium in the region $\{(r_i, r_j) : r_i \in (c\frac{1-\delta}{\delta}, \infty), r_j > \psi(r_i)\} \cap \{(r_i, r_j) : r_j \in (c\frac{1-\delta}{\delta}, \infty), r_i > \psi(r_j)\}$
3. Let $\psi(r_k) := \frac{-\delta r_k^2 + c(1+\delta) r_k}{\delta r_k - c(1-\delta)}$. (N, R) is the unique pure strategies Nash Equilibrium in the region $\{(r_i, r_j) : r_i \in (\frac{c}{\delta}, \infty), r_j < \psi(r_i)\}$
4. Let $\psi(r_k) := \frac{-\delta r_k^2 + c(1+\delta) r_k}{\delta r_k - c(1-\delta)}$. (R, N) is the unique pure strategies Nash Equilibrium in the region $\{(r_i, r_j) : r_j \in (\frac{c}{\delta}, \infty), r_i < \psi(r_j)\}$

i \ j	R	N
R	$p(r_i - c + \delta(r_j - c)) + (1-p)(1-\delta)(r_i - c)$, $(1-p)(r_j - c + \delta(r_i - c)) + p(1-\delta)(r_j - c)$	$r_i - c + \delta r_j$, $(1-\delta) r_j$
N	$(1-\delta) r_i$, $r_j - c + \delta r_i$	r_i , r_j

Figure 3: The game between i and j.

Intuitively, the lemmas organizes the (r_i, r_j) plane into several regions. In the convex hull comprised of large realizations of wealth for both parties, each party's dominant strategy is R. This is brought on by two motives. First, when i and j both have high

Figure 4: Pure-strategy Nash Equilibria in the (r_i, r_j) space

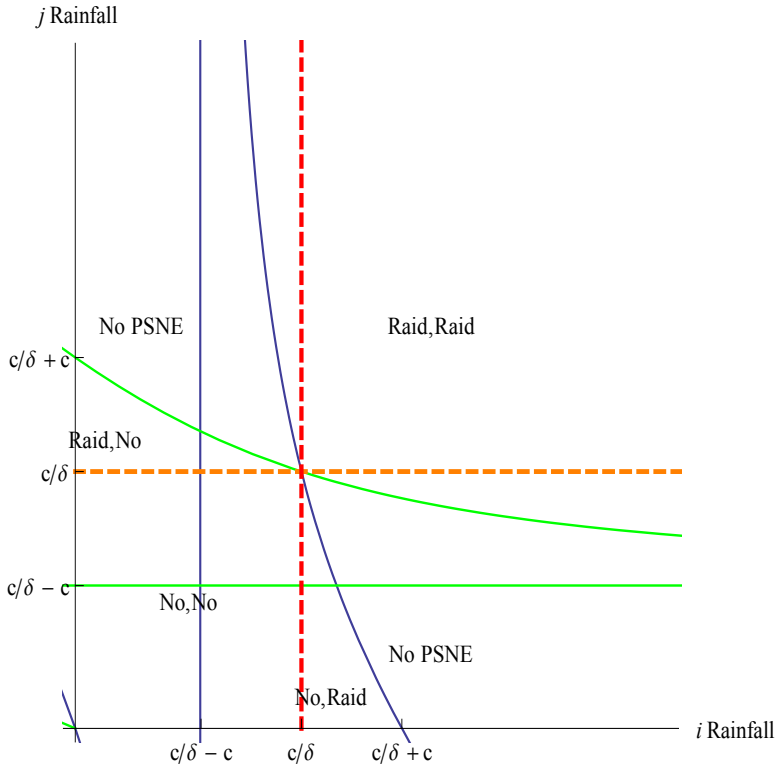

wealth, but i has relatively more, it is prone to raid because the probability of success in capturing some of j's wealth is relatively high. On the other hand, when j has relatively more, i prefers raiding because if it does win, it captures some of j's considerable wealth. The intuition behind the proposition that i wishes to raid j when j has higher wealth, comes from the 'rapacity effect', where i wishes to capture a fraction of j's larger resource pie. Whereas the intuition behind the finding that i wishes to raid when i has higher wealth comes from the 'relative strength' mechanism where i has more resources to build a stronger army and therefore a higher probability of victory against j.

2.3 A Sharing Rule

The possibility that conflict can be mitigated by the sharing of resources can be captured by a sharing-rule whereby each party shares a proportion ϕ of their wealth with the other party if and only if neither party raids the other. This changes the payoffs in the (N, N) portion of the game to be $(1-\phi)r_i + \phi r_j$ and $(1-\phi)r_j + \phi r_i$. That is, in the absence of any raids, party i receives $(1-\phi)$ of it's own resources, and a ϕ portion of party j's resources.

The modified game is presented in Figure 5. This sharing rule expands the region of the (N, N) Nash Equilibrium as can be seen in Figure 6,[3] and changes the best response functions in the following way:

Proposition 2.2 *For $\delta > \phi > \frac{\delta}{1+\delta}$ and $(r_i, r_j) \in \mathbb{R}^2_+$, the following are best response functions for agent k under a sharing-rule agreement:*

1. $BR_k(s_{-k} = N) = \begin{cases} R, & \text{if } r_{-k} > \frac{c-\phi r_k}{\delta-\phi} \\ N, & \text{else} \end{cases}$
2. *Let* $\psi(r_k) := \frac{-\delta r_k^2 + c(1+\delta) r_k}{\delta r_k - c(1-\delta)}$.

$BR_k(s_{-k} = R) = R$, *for all* (r_k, r_{-k}) *such that*

$$\{(r_k, r_{-k}) : r_k \in (c\frac{1-\delta}{\delta}, \infty), r_{-k} > \psi(r_k)\} \tag{3}$$

And $BR_k(s_{-k} = R) = N$, *for all* (r_k, r_{-k}) *such that*

$$\{(r_k, r_{-k}) : r_k \in (0, c\frac{1-\delta}{\delta})\} \cup \{(r_k, r_{-k}) : r_k \in (c\frac{1-\delta}{\delta}, \infty), r_{-k} < \psi(r_k)\} \tag{4}$$

The change in the best response functions, leads to an expansion of the (N, N) region of the Nash equilibrium.

Proposition 2.3 *The sharing-rule expands the Nash Equilibrium region of (No raid, No raid)*

The proof of this proposition, and a description of the Nash Equilibrium regions under the sharing rule can be found the Appendix A.2. Intuitively, the easier it is to trade and share the fruits of higher resources with your neighbors, the lower is the likelihood of conflict. This can be tested by focusing on conflicts across ethnic boundaries or countries.

3 Data

We combine data on rainfall, the spatial locations of conflicts, lighttime nights, and the locations of African ethnic groups. Our base observations are $0.5^\circ \times 0.5^\circ$ grid cells covering

[3]The figure restricts ϕ to values of $\delta > \phi > \frac{\delta}{1+\delta}$ for convenience in analysis

i \ j	R	N
R	$p(r_i - c + \delta(r_j - c)) + (1-p)(1-\delta)(r_i - c)$, $(1-p)(r_j - c + \delta(r_i - c)) + p(1-\delta)(r_j - c)$	$r_i - c + \delta r_j$, $(1-\delta)r_j$
N	$(1-\delta)r_i \quad , \quad r_j - c + \delta r_i$	$(1-\phi)r_i + \phi r_j$, $(1-\phi)r_j + \phi r_i$

Figure 5: The game with a sharing-rule

Figure 6: Pure-strategy Nash Equilibria in the (r_i, r_j) space with the Sharing-Rule

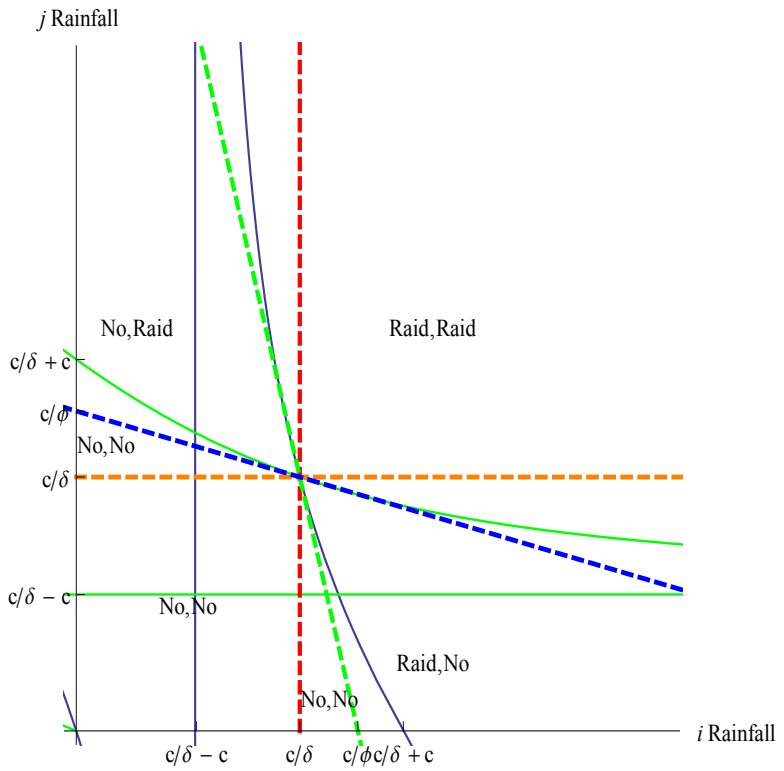

the whole of Africa. These are chosen to match the data on rainfall that are available in the well-known series from Matsuura and Willmott (2009). Hosted by the University of Delaware, these provide monthly temperature and rainfall at the degree resolution for the period 1900-2010.[4] Our main variable of interest is the mean annual rainfall experienced in each grid cell over the period 1992 to 2008. These data are commonly used in economic development (e.g. Dell et al. (2012)).

In order to merge spatial data on conflict to these rainfall points, we turn to the Uppsala Conflict Data Program (UCDP) / International Peace Research Institute, Oslo (PRIO) Armed Conflict Dataset, Version 4 - 2006. These data list conflicts and the years during which they occur. Initially coded by Gleditsch et al. (2002), these data report conflicts occurring between 1946 and 2008. To assign geographic coordinates to these conflicts, we add additional data, taken from Raleigh et al. (2006). For each conflict in the base PRIO data, these report a latitude/longitudecoordinate as well as a radius in kilometers. The circle defined by these numbers is taken as the area affected by the conflict, and we consider any rainfall point lying within this circle in year of conflict as experiencing conflict. Additional information on these data are provided by Raleigh et al. (2006) and Hallberg (2012). In particular, the latitude and longitude coordinate for a conflict is defined as the mid-point of all known locations of battles. The radius is constructed multiples of 50 km and encompasses all of these battle locations, except for sporadic violence far from the the remaining events.

We also consider the development implications of rainfall and conflict. We follow Michalopoulos and Papaioannou (2013) and Henderson et al. (2012) in using night-time lights as a proxy. Luminosity data are taken from the Defense Meteorological Satellite Program's Operational Linescan System. Major advantages of these data include their arbitrary divisibility, their consistency across multiple political jurisdictions, their high spatial resoultion, and their availability given the weaknesses of lack official data on African economic activity (Jerven, 2013). Henderson et al. (2012) provide additional information on the data. These data are constructed as an annual average of satellite images of the earth taken daily between 20:30 and 22:00 local time. The raw data are at a 30 second resolution, which implies that each pixel in the raw data is roughly one square kilometer. We average over pixels within a rainfall point. The raw luminosity data for each pixel is reported as a six-bit integer ranging from 0 to 63.

To code whether two rainfall points belong to the territories of different ethnic groups,

[4] See *http://climate.geog.udel.edu/~climate/*.

we use the ethnic map of Africa from Murdock (1959). This reports the locations of more than 800 African ethnic groups as polygons, making it easy to assign a rainfall point to the polygon into which it falls. This map has been used by several researchers on African development, including Michalopoulos and Papaioannou (2013), Michalopoulos and Papaioannou (2011) and Nunn and Wantchekon (2011).

3.1 Summary Statistics

Table 1: Summary Statistics

Variable	Mean	Maximum	Minimum	Standard Deviation
Prob(region i&j in the same conflict)	0.46	1.00	0.00	0.50
Average Rainfall (1998 to 2008)	52.70	319.45	0.08	48.88
Light-Density Index	0.29	57.21	0.00	1.72
Distance between region i&j (km)	329.03	500.00	44.51	117.36

Table 1 reports summary statistics for key variables used in the empirical analysis below.

4 Estimation Strategy

The theoretical model allows us to divide the conflict-resources space into four distinct Nash Equilibrium regions. When there are low resources for both parties, there is a lower probability of conflict as neither party has resources to build an army and there is no wealth to appropriate from ones neighbor. On the other hand, having a high amount of resources for either party leads to more conflict, and this is especially true when both parties have high levels of resources.

In order to capture this pattern produced by the Nash regions in Figure 4, one can use the following regression specification:

$$conflict_{ij} = \beta_0 + \beta_1 \mathbb{1}_{r_i > r^c} + \beta_2 \mathbb{1}_{r_j > r^c} + \beta_3 \mathbb{1}_{r_i > r^c} * \mathbb{1}_{r_j > r^c} + \epsilon_{ij} \tag{5}$$

In this formulation, r^c represents the cutoffs in Figure 4 separating the Nash regions. As a region's own resources r_i crosses the cutoff r^c, we enter a different Nash region.

Therefore, β_0 captures the (No, No) region in the south-west section of Figure 4 where neither party raids. Similarly, $\beta_0 + \beta_1$ captures the north-western quadrant of the graph which is represented by a $(Raid, No)$ region and a no-pure strategy equilibrium region. $\beta_0 + \beta_2$ corresponds to the $(No, Raid)$ and no-pure strategy region in the south-east section of the graph, and $\beta_0 + \beta_1 + \beta_2 + \beta_3$ captures the $(Raid, Raid)$ quadrant of the figure. Given the models predictions, we should therefore expect $\beta_1 \geq 0$, $\beta_2 \geq 0$ and $\beta_1 + \beta_2 + \beta_3 > 0$.

For the empirical exercise, long-run rainfall over a ten year period will be used to represent the accumulation of resources. While the amount of rainfall is admittedly a random occurrence, there may be reason to control for various factors that otherwise influence the likelihood of conflict in Africa. These controls include (for both points i and j) latitude and longitude, measures of land quality, malaria prevalence, humidity, population density, ruggedness and the distance between the two points. Furthermore, we also restrict attention to the variation within continuous regions by including fixed effects for Agro-Ecological Zones (AEZ), and latitude-longitude grids of various sizes.[5]

In order to estimate Equation 5 it is necessary to identify the cutoff r^c. One simple approach would be to just use the median level of rainfall. While all our results are consistent with using the median as a cutoff, there is no reason to believe the median is the right threshold. The literature on structural breaks has made large headways in identifying such cutoffs in various contexts (Bai, 1997a,b, 2010; Bai and Perron, 1998; Gonzalo and Pitarakis, 2002; Gonzalo and Wolf, 2005; Hansen, 2000). Theses papers propose that the cutoff can be estimated by using a search algorithm that identifies the threshold which minimizes the residual sum of squares of the model, or alternatively maximizes the partial R-squared for the the variable of interest. Under a correctly specified model, this process leads to a consistent estimate of the cutoff and the parameters of interest.

While a lot of this literature focuses on structural breaks in time-series data, there are applications using cross-sectional micro-data (Card et al., 2008), which argue that likelihood ratio (LR) tests under the null of no-structural breaks doesn't allow for conventional hypothesis testing, and instead suggests alternative methods that do not suffer from the drawbacks of such LR tests (Gonzalo and Wolf, 2005). The advantage of having a large micro-sample is that we can use a split-sample approach - while one portion of the sample is used to identify the cutoff, the rest is utilized in running the regression of interest

[5]While the main tables include grids of 7 degrees by 7 degrees, the results are shown to be robust to using other grid sizes

taking the cutoff as given (Angrist et al., 1999; Angrist and Krueger, 1995). Due to the independence of the sub-samples, the cutoff has a standard distribution under the null. One application of this can be found in Card et al. (2008), where they use two-thirds of the sample to identify a threshold and the remaining one-third to identify the coefficients of interest. Similarly, Gonzalo and Wolf (2005) use the intuition behind Politis and Romano (1994) to propose using many randomly selected sub-samples to describe the distribution of cutoffs and coefficients of interest.

In keeping with the literature, therefore, the following empirical strategy is used. Two-thirds of the data is randomly selected, upon which the search algorithm is performed to identify the cutoff which minimizes the residual sum of squares. An example of this can be seen in Figure 11, which identifies the value of rainfall-cutoff for which the R-squared is maximized in Equation 5. The remaining one-third is then used to identify the coefficients in the equation. This process is repeated with various randomly selected sub-samples to describe the distribution of the cutoffs and the parameters estimated. In our case, however, the process of repeatedly picking different sub-samples did not greatly affect the estimates, largely because there was little to no change in the optimal cutoff across iterations (Figure 12). The results reported, therefore, are of a randomly selected iteration, and the distribution of the coefficients of interest across iterations are shown in Figure 13 - 15.

While identifying the cutoff is necessary for estimating β_1, β_2 and β_3, it is also an informative parameter in itself since it represents the threshold amount of resources which pushes parties into conflict. As theory suggests, this threshold may be lower for regions which either have a lower cost of conflict, or higher potential returns to conflict. Facilitation of trade or any other sharing-rules may, alternatively, raise the threshold necessary for the outbreak of conflict. Figures 7 to 9 show the threshold values for for different sub-samples in the data. Regions that are closer to each other (less than 250kms apart), may have lower costs of raiding, and the threshold amount of rainfall is lower for these subsamples than it is for regions further away (between 250 and 500kms). Furthermore, geographically similar neighbors are less likely to attack each other since regions that have the same type of vegetation have a higher threshold than those that are different. Lastly, one can look at the subsample of pairs that lie within countries and compare that to the pairs that are in different countries. While the difference is not large, being in the same country does raise the threshold amount of rainfall, possibly due to greater trade opportunities within a nation.

One additional issue is that of the estimation of standard errors. A standard result in the structural break literature is that the sampling error in the break can be ignored when estimating the size of the break (Bai, 1997b; Card et al., 2008). Given the iterative nature of the split-sample approach, it is possible to obtain a distribution of the coefficients of interest (Figures 13 to 15). However, as the results section will show this produces extremely tight standard errors due to a very precisely estimated cutoff-value (Figure 12), and a more conservative approach may be pertinent. Given the possibility of spatial correlation in the errors, the approach we use is to cluster the standard errors at various geographic levels. The data consists of points of a size spanned by 0.5x0.5 degree in latitude and longitude, matched to each of it's neighboring points within a 500km radius. Standard errors can therefore be clustered at that point level, or two-way clustered errors can be calculated for the point and its neighboring region. Estimates that allow for a greater degree of spatial correlation can be obtained by calculating errors at latitude-longitude grids of larger sizes, ranging from a 1x1 degree grid, to a more conservative 3x3 degree grid which consists of thirty-six adjacent points and spans approximately 111.5 thousand square kilometers near the equator.

The cutoffs not only allow for the estimation of Equation 5, but also the estimation of the size of the discontinuity at each boundary. In doing so, one can rely on the Regression Discontinuity (RD) literature to identify how the probability of conflict changes at each threshold. This will be done using the latest methods developed by Calonico et al. (2014), which calculates the optimal bandwidths, and provides a robust bias-corrected estimate of the coefficients and standard errors. The RD method can be used for six-different results. The first is just to see what happens to conflict when the region's own rainfall crosses the threshold, whereas the second looks at the effect of the neighboring region's rainfall at the cutoff. However, this captures an average of the effects along four different discontinuities. In crossing from the south-west to the south-east region of Figure 4, one can look at the discontinuity along a region's own rainfall after conditioning the subsample to be such that the neighboring region's rainfall lies below the cutoff (and thus the entire subsample lies in the southern-region of the figure). Similarly, in crossing from the north-west to the north-east region of Figure 4 one can study the discontinuity along a region's rainfall conditioning on the sub-sample such that the neighboring region's rainfall lies above the threshold (and lies entirely in the northern portion of the figure). This can then be done for the two discontinuities driven by the neighboring region's rainfall crossing the threshold as well.

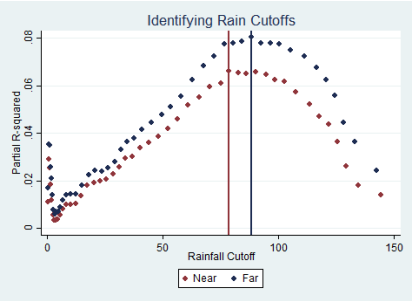

Figure 7: By Distance Between i&j pairs - Near points have a cutoff of 78.595 whereas far points have a cutoff of 88.126

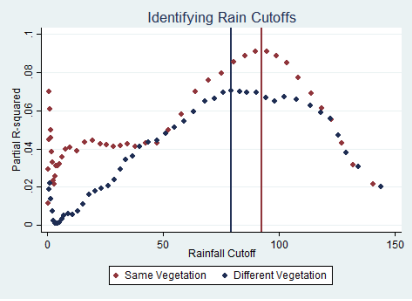

Figure 8: By Vegetation Zones - Different vegetation has a cutoff of 79.2 whereas same vegetation has a cutoff of 89.38

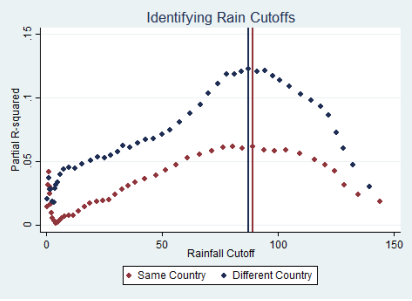

Figure 9: By Country - Different country has a cutoff of 87.22 whereas same country has a cutoff of 88.87

Structural Break Search-Algorithm. These figures represent the search-algorithm outlined in the paper, that identify the structural breaks.

5 Results

In this section, we present and discuss empirical evidence in support of the model developed in section 2. The analysis is carried out in multiple stages as discussed in section 4 above.

5.1 Joint Conflict

We start by showing a heat map of joint conflict between points i and j as function of the 10 year moving average of rainfall in point i and the 10 year moving average of rain in point j. The heat map, shown in Figure 10, bears remarkable resemblance to the graph depicting the model predictions in Figure 2. That is, the region adjacent to the origin shows little to no likelihood of joint conflict; while the upper-right quadrant of the heat map corresponds to the highest likelihood of joint conflict, as predicted by the model. The no-conflict region at the origin extends along both the x and y axes until a distinct boundary, beyond which the likelihood of conflict jumps up discontinuously. Specifically, a high degree of inequality between rain in i and j (e.g., high rain i and low rain j) causes a high probability of joint conflict. This high probability of conflict diminishes as the inequality diminishes (i.e. rain j rises to closer to the high rain i level), but then jumps up again as we approach equally high rain levels for both i and j (i.e., as we approach the upper-right quadrant).

Figure 10: Heat Map of the Probability of Conflict by Long-Run Rainfall

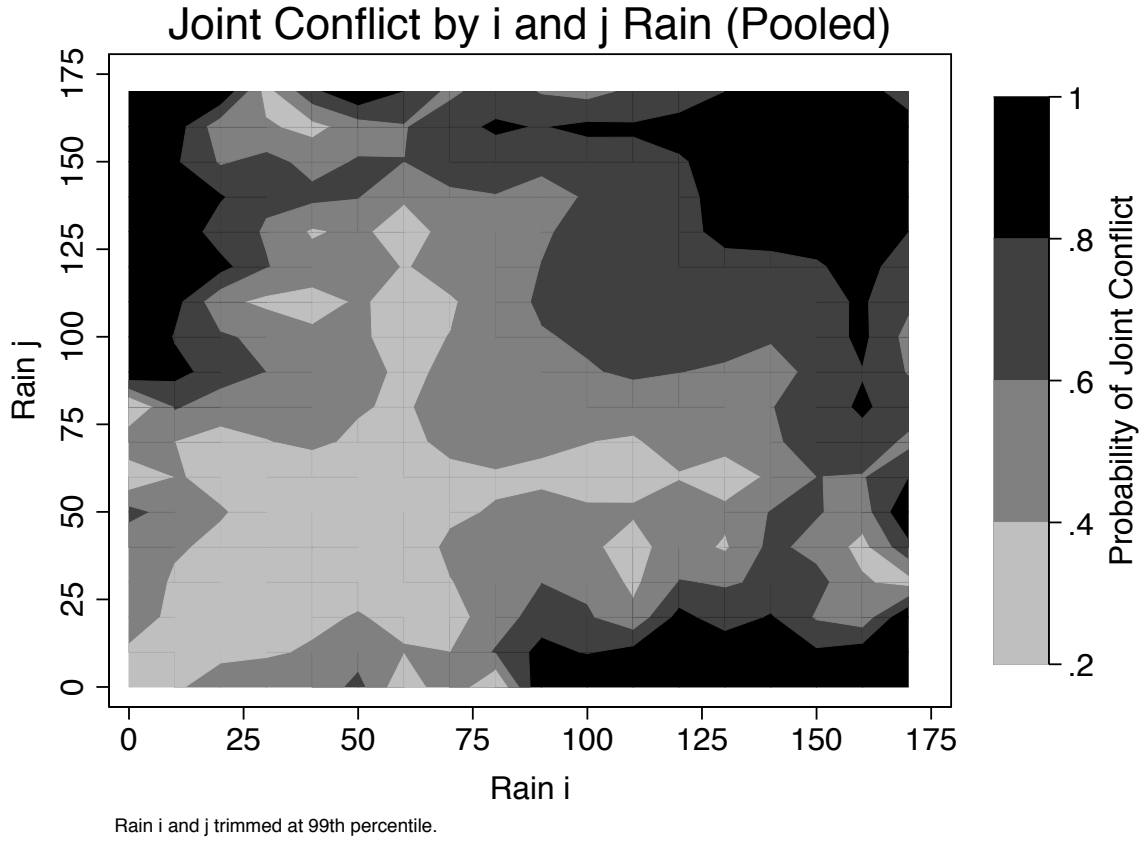

Using the procedure discussed in section 4, we estimate the cutoff level of rainfall above which the probability of joint conflict jumps up discontinuously to be 88.667 (reported in the last row of Table 2), which corresponds to the discontinuity depicted in Figure 10 quite well. The distribution around this estimate of the cutoff for the full sample of data is shown in Figures 11 and 12. Using this cutoff value, we then regress the probability of a joint conflict between point i and j on dummies for rain i being above the cutoff, rain j being above the cutoff, and both rain i and rain j being above the cutoff. As discussed in section 4, we estimate four different specifications with varying levels of controls and fixed effects. The results of these regressions are presented in Table 2 with the controls and fixed effects denoted for each columns in the rows below the estimated coefficients and standard errors.

Table 2 shows that rain i falling above the cutoff increases the probability of a joint conflict, as does rain j falling above the cutoff. Furthermore, as predicted by the model,

Figure 11: Finding the Optimal Cutoff

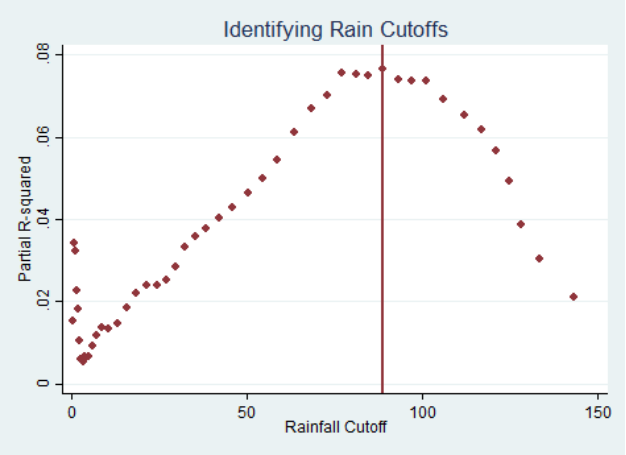

Figure 12: Distribution of Optimal Cutoffs

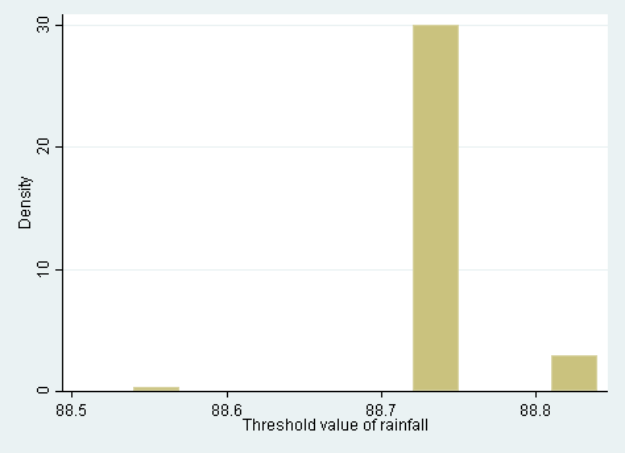

The optimal cutoff is estimated using the search algorithm described in the empirical section, and was found to be 88.667 for the full sample. The procedure outlined in the estimation section was repeated where a one-third random sample was used to estimate the cutoff, and the remaining two-third random sample was used to identify the coefficients. The lower panel shows the distribution of optimal cutoffs based on this procedure.

Figure 13: Rain $i >$ cutoff

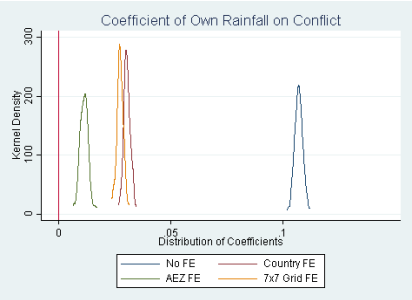

Figure 14: Rain $j >$ cutoff

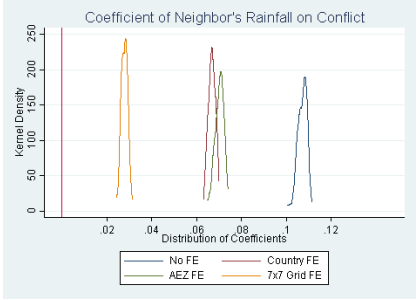

Figure 15: Rain i&j $>$ cutoff

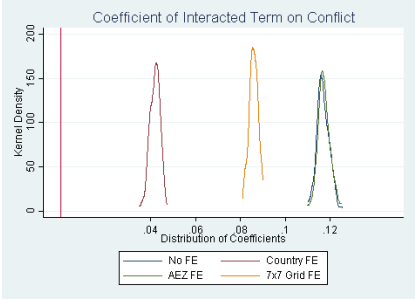

BOOTSTRAPPED ESTIMATES. The procedure outlined in the estimation section was repeated where a one-third random sample was used to estimate the cutoff, and the remaining two-third random sample was used to identify the coefficients. This figure shows the distribution of coefficients from that procedure.

the probability of a joint conflict increases further when both rain i and rain j fall above the cutoff. These results verify that the patterns in the heat map in Figure 10, showing the lowest probability of joint conflict in the lower-left quadrant, a high probability of conflict in the upper-left and lower-right quadrants and the highest probability of conflict in the upper-right quadrant, are indeed statistically significant. The results are robust across the different specifications including controls for both points i and j, along with fixed effects

Table 2: The Effect of Rainfall Crossing Certain Cutoffs on Conflict

Dependent Variable: Probability(Region i&j in same conflict between 1998-2008)				
$\mathbb{1}(rain_i > rain^{cutoff})$	**0.114**	**0.134**	**0.0358**	**0.0501**
SE cluster: Point *i*	(0.0132)***	(0.0134)***	(0.0141)**	(0.00903)***
2 by 2 grid	(0.0410)***	(0.0376)***	(0.0342)	(0.0197)**
2-way: Point i&j	(0.0167)***	(0.0160)***	(0.0272)	(0.0287)*
$\mathbb{1}(rain_j > rain^{cutoff})$	**0.111**	**0.132**	**0.0916**	**0.0557**
SE cluster: Point *i*	(0.0105)***	(0.00911)***	(0.00822)***	(0.00475)***
2 by 2 grid	(0.0326)***	(0.0264)***	(0.0227)***	(0.0117)***
2-way: Point i&j	(0.0166)***	(0.0159)***	(0.0192)***	(0.0244)**
$\mathbb{1}(rain_i \& rain_j > rain^{cutoff})$	**0.124**	**0.0934**	**0.0835**	**0.0391**
SE cluster: Point *i*	(0.0152)***	(0.0137)***	(0.0122)***	(0.00752)***
2 by 2 grid	(0.0524)**	(0.0427)**	(0.0345)**	(0.0191)**
2-way: Point i&j	(0.0212)***	(0.0190)***	(0.0209)***	(0.0217)*
R-squared	0.077	0.192	0.227	0.612
Fixed Effects	None	None	AEZ	Grid 7 by 7
Controls - point i	None	All	All	All
Controls - point j	None	All	All	All
Observations		802,553		
Mean dependent variable		0.455		
Estimated rain cutoff		88.667		

Notes: Regressions of ever being involved in the same conflict over a ten year period (1998 to 2008) on rainfall for the region and neighboring region being above an estimated cutoff.
Search algorithm for rainfall cutoffs described in the empirical section and estimated cutoff is reported in the table above. One-third of the sample (1604623 observations) were randomly selected for the search procedure.
Observations including region i&j pairs where region *j* is within 500 kilometers of region i- data is averaged over a ten year period between 1998 and 2008.
Controls include (for both points *i* and j) latitude, longitude, ruggedness index, land quality index, humidity, malaria, population density, and a quadratic of the distance between two points
Fixed effects include Agro-Ecological Zones (AEZ), and latitude-longitude 7 by 7 degree geographic grids
Standard errors clustered at (a) Point i-level, (b) Point i&j 2-way cluster, (c) latitude-longitude grids - 2 by 2 grid consisting of sixteen adjacent points and spanning approximately 50 thousand square km

for agro-ecological zones (AEZ) or squares of the geospatial grid 7 degrees latitude by 7 degrees longitude in size. Tthe statistical significance of the results is generally preserved when clustering standard errors at larger squares of the point *i* geospatial grid as well as two way clustering by squares in both the *i* and *j* geospatial grids. Lastly, Table 3 reports

Table 3: Variation within Different Latitude-Longitude Grids

Dependent Variable: Probability(Region i&j in same conflict between 1998-2008)				
Grid Fixed Effects	Grid 4 by 4	Grid 5 by 5	Grid 6 by 6	Grid 7 by 7
$\mathbb{1}(rain_i > rain^{cutoff})$	**0.0207**	**0.0195**	**0.0436**	**0.0501**
SE cluster: 1 by 1 grid	(0.0112)*	(0.0123)	(0.0131)***	(0.0148)***
2 by 2 grid	(0.0151)	(0.0146)	(0.0182)**	(0.0197)**
3 by 3 grid	(0.0181)	(0.0172)	(0.0207)**	(0.0249)**
$\mathbb{1}(rain_j > rain^{cutoff})$	**0.0365**	**0.0350**	**0.0371**	**0.0557**
SE cluster: 1 by 1 grid	(0.00692)***	(0.00767)***	(0.00720)***	(0.00802)***
2 by 2 grid	(0.0104)***	(0.0113)***	(0.0122)***	(0.0117)***
3 by 3 grid	(0.0134)***	(0.0142)**	(0.0139)***	(0.0148)***
$\mathbb{1}(rain_j \& rain_j > rain^{cutoff})$	**0.0388**	**0.0509**	**0.0638**	**0.0391**
SE cluster: 1 by 1 grid	(0.0119)***	(0.0122)***	(0.0125)***	(0.0124)***
2 by 2 grid	(0.0187)**	(0.0188)***	(0.0215)***	(0.0191)**
3 by 3 grid	(0.0245)	(0.0242)**	(0.0255)**	(0.0253)
R-squared	0.709	0.701	0.684	0.675
Fixed Effects	Grid 4 by 4	Grid 5 by 5	Grid 6 by 6	Grid 7 by 7
Controls - point i	All	All	All	All
Controls - point j	All	All	All	All
Observations	802,553			
Mean dependent variable	0.455			
Estimated rain cutoff	88.667			

Notes: Regressions of ever being involved in the same conflict over a ten year period (1998 to 2008) on rainfall for the region and neighboring region being above an estimated cutoff.
Fixed Effects include different latitude-longitude degree grids. For example, a 4 by 4 grid consists of 64 adjacent data points of size 0.5 by 0.5 degrees each
Search algorithm for rainfall cutoffs described in the empirical section and estimated cutoff is reported in the table above. One-third of the sample (1604623 observations) were randomly selected for the search procedure.
Observations including region *i*&*j* pairs where region *j* is within 500 kilometers of region i- data is averaged over a ten year period between 1998 and 2008.
Controls include (for both points *i* and j) latitude, longitude, ruggedness index, land quality index, humidity, malaria, population density, and a quadratic of the distance between two points
Standard errors clustered at latitude-longitude degree grids - For example, a 2 by 2 grid consisting of sixteen adjacent points.

robustness results from specifications including fixed effects corresponding to geospatial grid squares of varying sizes as well as standard errors clustered in i grid squares of varying sizes. The general pattern and overall significance of the results are preserved.

Next, having verified the differences in the probability of joint conflict across the four quadrants depicted in Figure 10, we test whether the relationships between the probability of joint conflict and rainfall in points i and j are in fact discontinuous at the cutoffs estimated. We begin by presenting graphical depictions of a regression discontinuity in conflict as a function of rainfall. Figures 16 and 17 show evidence of discontinuities in the probability of joint conflict as functions of both rainfall at point i (Figure 16) and rainfall at point j (Figure 17). Figures 18 and 19 repeat the exercise, restricting the sample to observations for which rainfall is below the neighbor's rainfall cutoff, whereas Figures 20 and 21 restrict it to being above the neighbors cutoff. For example, Figure 18 depicts the discontinuity in the probability of joint conflict as a function of own rainfall, conditional on rain j being below the cutoff value; while Figure 19 depicts the discontinuity as a function of rain j conditional on rain i being below the cutoff value. Similarly, Figures 20 and 21 repeats this exercise conditioning on the non-depicted running variable being *above* the cutoff value for rainfall.

Figure 16: RD at the Rain i-cutoff

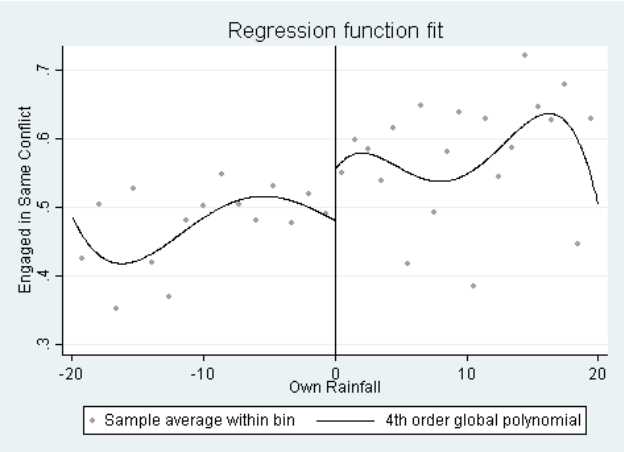

Figure 17: RD at the Rain j-cutoff

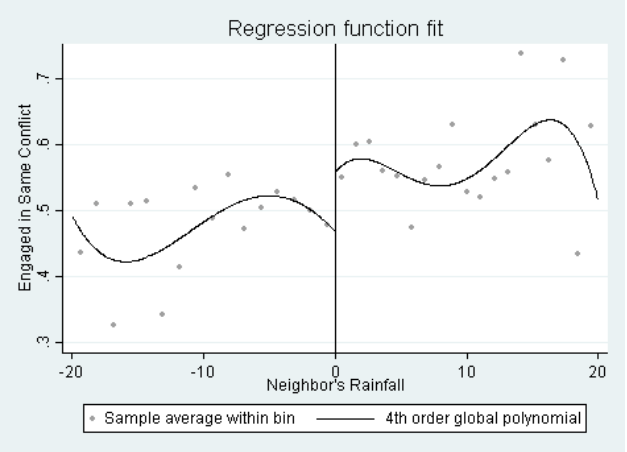

RD graphs of being engaged in the same conflict on rainfall. Graphs were produced using the Calonico, Cattaneo and Titunik (2014) procedure of identifying the optimal bin sizes.

Table 4 reports results from the estimation of regression discontinuity specifications analogous to the exercises depicted in Figures 16 through 21. The results show that the discontinuities in the probability of joint conflict at the cutoff values in rainfall, both con-

Figure 18: RD at the Rain i-cutoff, Rain j below cutoff

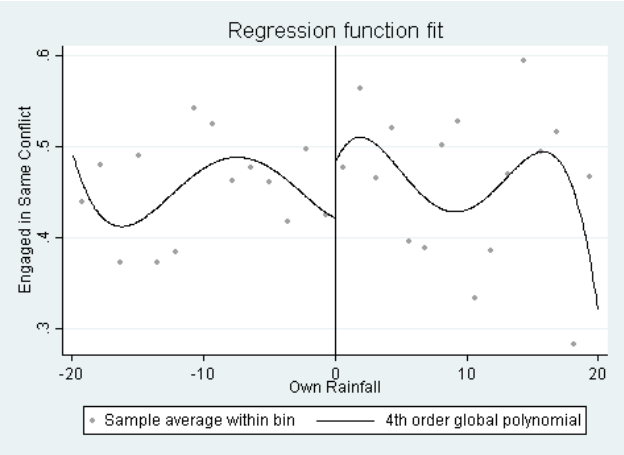

Figure 19: RD at the Rain j-cutoff, Rain i below cutoff

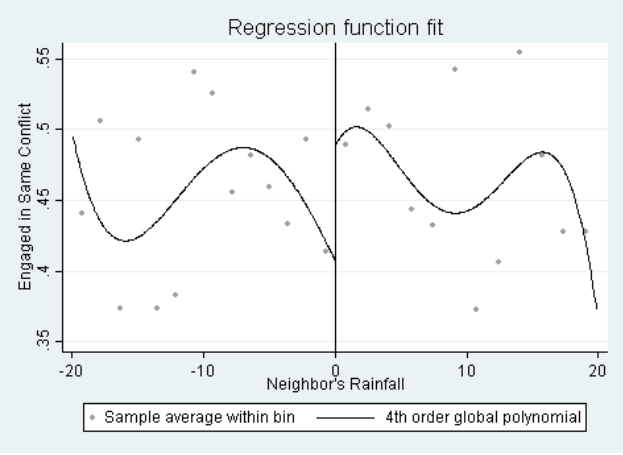

RD graphs of being engaged in the same conflict on rainfall. Graphs were produced using the Calonico, Cattaneo and Tituinik (2014) procedure of identifying the optimal bin sizes.

Figure 20: RD at the Rain i-cutoff, Rain j above cutoff

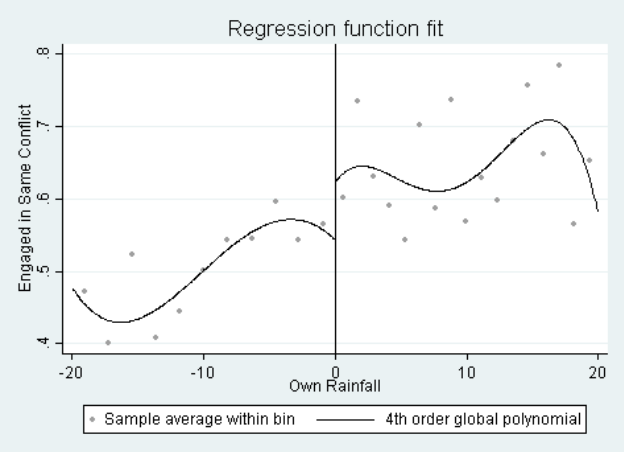

Figure 21: RD at the Rain j-cutoff, Rain i above cutoff

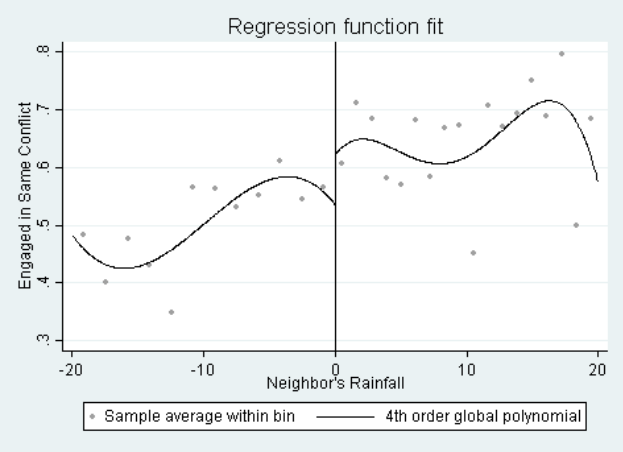

RD graphs of being engaged in the same conflict on rainfall. Graphs were produced using the Calonico, Cattaneo and Tituinik (2014) procedure of identifying the optimal bin sizes.

ditional and unconditional, are indeed statistically significant. We interpret these large and significant discontinuities in the probability of joint conflict as strong evidence in support of the model developed in section 2 and its predictions.

Table 4: Regression Discontinuity Tables: Conflict on Rain

Panel A: At rain i-cutoff P(i&j in same conflict)	Full Sample	Subsample: For $\mathbb{1}(r_j > r^c)$	Subsample: For $\mathbb{1}(r_j < r^c)$
RD Estimate	0.0764	0.0902	0.0836
At Rain i-cutoff	(0.0114)***	(0.0153)***	(0.0152)***
Observations in BW	41,982	23,903	25,126
Conventional p-value	0	0	0
Robust p-value	0	0	0
Bias Corrected p-value	0	0	0
Order Loc.Poly.	1	1	1
Order Bias Correction	2	2	2
BW Loc. Poly.	5.266	6.039	6.142
BW Bias Correction	15.42	17.25	15.96
Panel B: At rain j-cutoff P(i&j in same conflict)	Full Sample	Subsample: For $\mathbb{1}(r_i > r^c)$	Subsample: For $\mathbb{1}(r_i < r^c)$
RD Estimate	0.0856	0.0835	0.0911
At Rain j-cutoff	(0.0116)***	(0.0156)***	(0.0152)***
Observations in BW	39,238	22,548	24,917
Conventional p-value	0	0	0
Robust p-value	0	0	0
Bias Corrected p-value	0	0	0
Order Loc.Poly.	1	1	1
Order Bias Correction	2	2	2
BW Loc. Poly.	4.973	5.661	6.115
BW Bias Correction	15.44	17.66	16.42

Regression Discontinuity estimates calculated using Calonico, Cattaneo and Titunik (2014) bandwidth selection and bias correction procedures.
The p-values for the bias-corrected and robust methods are presented, as well as the size of the optimal bandwidth, and the bandwidth for bias correction
Dependent variable: Region i&j ever engaged in the same conflict in a ten-year period between 1998 and 2008
Running variable: Panel A - own rainfall, normalized to 0 using estimated rainfall cutoff of 88.667. Panel B - rainfall of neighboring region, normalized to 0 at cutoff
Results reported for different subsamples: (a) Full sample includes the two-thirds of the sample not used to estimate the cutoff, (b) Subsample: for other running variable being above cutoff, and (c) Subsample for other running variable being below its cutoff

5.2 Other Resources

Although we chose to emphasize rainfall as a proxy for long-run resource accumulation, largely due to the ubiquitousness of agricultural activity across Africa and the random

nature of climate realizations, we can demonstrate a strong degree of robustness and consistency when testing the predictions of the model using data on other resources common to various parts of the continent. Specifically, we repeat the analysis presented in Figure 10 and Table 2 using the presence of oil, agricultural productivity of the land, and presence of diamonds as our measures of resource richness.

Figure 22: Heat Map of the Probability of Conflict by the Presence of Oil Fields

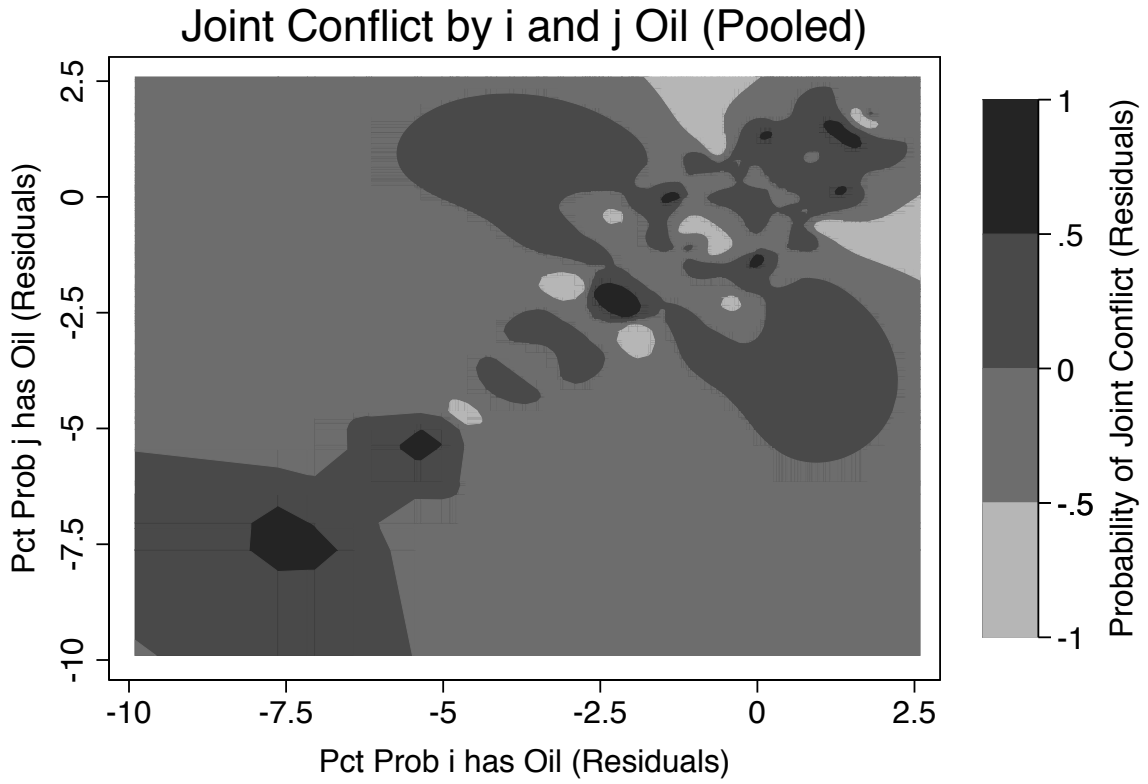

Figure 22 presents a heat map depicting joint conflict as a function of the probabilities that points i and j contain oil fields[6]. Figure 23 depicts joint conflict as a function of land quality in i and j, and Figure 24 depicts joint conflict as a function of the probability that i and j contain deposits of diamonds. All three figures show the upper-right quadrant as most conflict intense region with discontinuous drops in conflict intensity as we move from the upper-right to the upper-left and from the upper-right to the lower-right. Ad-

[6]Note that because the resource variables used in Figures 22 and 24 are binary, we use residuals from a regression of these binary resource variables on AEZ fixed effects to graphically represent the relative degree of resource richness.

Figure 23: Heat Map of the Probability of Conflict by Land Quality

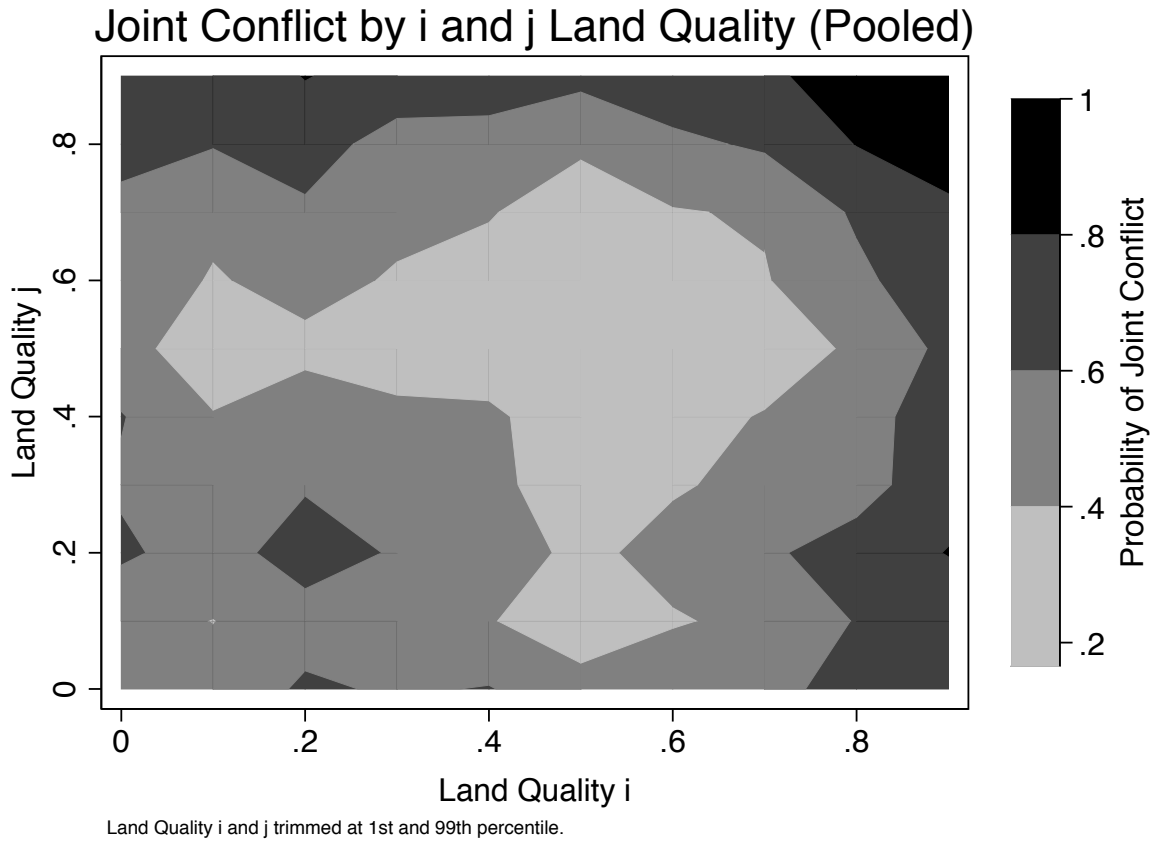

ditionally, all three heat maps show relatively less conflict intensity in regions depicting balanced resource scarcity. [7]

Tables 5, 6, and 7 present analogous regression results to those depicted in Table 2. With few exceptions, the regression estimates indicate that the patterns identified in the respective heat maps are statistically significant. That is, conflict intensity is lowest when both *i* and *j* are resource poor, higher when either *i* or *j* is considerably more resource rich than the paired point, and highest when both *i* and *j* are resource rich. Artifacts deriving from the uncommonness of these other resources and the discrete nature of the measured variation in these resources notwithstanding, we interpret these results as further evidence in support of the predictions of the model. We also conduct a sort of falsification exercise to verify that less easily appropriated resources (e.g., nonlooatable diamonds)

[7] Oil is a notable exception in that there appears to be a region of intense conflict in the lower-left quadrant. We attribute this to the rarity of oil by geographic space in the sample, such that less 5% of *i* squares on the grid contain oil fields. Accordingly, we do not emphasize this result very strongly.

Table 5: Conflict Intensity and Oil Fields

Dependent Variable: Probability(Region i&j in same conflict between 1998-2008)				
Oil-i	0.0854	-0.0645	0.0208	0.0524
SE cluster: Point *i*	(0.0245)***	(0.0264)**	(0.0272)	(0.0125)***
2 by 2 grid	(0.0593)	(0.0636)	(0.0652)	(0.0196)***
2-way: Point i&j	(0.0235)***	(0.0249)***	(0.0271)	(0.0359)
Oil-j	0.0854	-0.0645	0.00295	0.00729
SE cluster: Point *i*	(0.0117)***	(0.0105)***	(0.0102)	(0.00391)*
2 by 2 grid	(0.0387)*	(0.0366)*	(0.0350)	(0.0119)
2-way: Point i&j	(0.0235)***	(0.0249)***	(0.0269)	(0.0314)
Oil-i x Oil-j	0.0115	0.0987	0.0459	0.0307
SE cluster: Point *i*	(0.0192)	(0.0193)***	(0.0194)**	(0.0125)**
2 by 2 grid	(0.0501)**	(0.0504)***	(0.0500)**	(0.0325)
2-way: Point i&j	(0.0257)***	(0.0261)***	(0.0259)***	(0.0290)*
R-squared				
Fixed Effects	None	None	AEZ	Grid 7 by 7
Controls - point i	None	All	All	All
Controls - point j	None	All	All	All
Observations			802,553	
Mean dependent var			0.455	

Notes: Regressions of ever being involved in the same conflict over a ten year period (1998 to 2008) on whether or not the region has an oil (or oil and gas) field.
Observations including region i&j pairs where region *j* is within 500 kilometers of region i- data is averaged over a ten year period between 1998 and 2008.
Controls include (for both points *i* and j) latitude, longitude, ruggedness index, land quality index, humidity, malaria, population density, and a quadratic of the distance between two points
Standard errors clustered at latitude-longitude degree grids - For example, a 2 by 2 grid consisting of sixteen adjacent points.

Table 6: Conflict Intensity and Land Quality

Dependent Variable: Probability(Region i&j in same conflict between 1998-2008)				
$\mathbb{1}(LandQuality_i > cutoff)$	0.248	0.138	0.0605	-0.0164
SE cluster: Point *i*	(0.0247)***	(0.0234)***	(0.0229)***	(0.0116)
2 by 2 grid	(0.0538)***	(0.0493)***	(0.0479)	(0.0184)
2-way: Point i&j	(0.0262)***	(0.0245)***	(0.0272)**	(0.0393)
$\mathbb{1}(LandQuality_j > cutoff)$	0.250	0.141	0.0770	-0.000313
SE cluster: Point *i*	(0.00955)***	(0.00815)***	(0.00785)***	(0.00457)
2 by 2 grid	(0.0317)***	(0.0265)***	(0.0243)***	(0.0135)
2-way: Point i&j	(0.0261)***	(0.0244)***	(0.0257)***	(0.0364)
$\mathbb{1}(LandQuality_{i\&j} > cutoff)$	-0.0458	0.0420	0.0647	0.0271
SE cluster: Point *i*	(0.0190)**	(0.0174)**	(0.0157)***	(0.00788)***
2 by 2 grid	(0.0469)	(0.0407)	(0.0335)*	(0.0145)*
2-way: Point i&j	(0.0262)*	(0.0238)*	(0.0262)**	(0.0392)
R-squared	0.077	0.192	0.227	0.612
Fixed Effects	None	None	AEZ	Grid 7 by 7
Controls - point i	None	All	All	All
Controls - point j	None	All	All	All
Observations		802,553		
Mean dependent var		0.455		
Land quality cutoff		0.785		

Notes: Regressions of ever being involved in the same conflict over a ten year period (1998 to 2008) on whether or not land quality is above the cutoff.
The estimation of the cutoff is highlighted in the empirical section.
Observations including region i&j pairs where region *j* is within 500 kilometers of region i- data is averaged over a ten year period between 1998 and 2008.
Controls include (for both points *i* and j) latitude, longitude, ruggedness index, land quality index, humidity, malaria, population density, and a quadratic of the distance between two points
Standard errors clustered at latitude-longitude degree grids - For example, a 2 by 2 grid consisting of sixteen adjacent points.

Table 7: Conflict Intensity and Lootable Diamonds

Dependent Variable: Probability(Region i&j in same conflict between 1998-2008)				
Lootable Diamonds-i	0.143	0.171	0.100	0.0175
SE cluster: Point *i*	(0.0305)***	(0.0272)***	(0.0258)***	(0.0135)
2 by 2 grid	(0.0522)***	(0.0456)***	(0.0412)**	(0.0195)
2-way: Point i&j	(0.0313)***	(0.0278)***	(0.0328)***	(0.0366)
Lootable Diamonds-j	0.143	0.171	0.131	0.0391
SE cluster: Point *i*	(0.00742)***	(0.00588)***	(0.00506)***	(0.00381)***
2 by 2 grid	(0.0265)***	(0.0205)***	(0.0165)***	(0.0117)***
2-way: Point i&j	(0.0313)***	(0.0278)***	(0.0310)***	(0.0335)
Lootable Diamonds-i& j	0.0658	-0.000336	0.0205	0.0177
SE cluster: Point *i*	(0.0184)***	(0.0159)	(0.0153)	(0.0144)
2 by 2 grid	(0.0387)*	(0.0308)	(0.0282)	(0.0255)
2-way: Point i&j	(0.0249)***	(0.0214)	(0.0286)	(0.0344)
R-squared				
Fixed Effects	None	None	AEZ	Grid 7 by 7
Controls - point i	None	All	All	All
Controls - point j	None	All	All	All
Observations		802,553		
Mean dependent var		0.455		

Notes: Regressions of ever being involved in the same conflict over a ten year period (1998 to 2008) on whether or not the region has lootable diamond mines.
Observations including region i&j pairs where region *j* is within 500 kilometers of region i- data is averaged over a ten year period between 1998 and 2008.
Controls include (for both points *i* and j) latitude, longitude, ruggedness index, land quality index, humidity, malaria, population density, and a quadratic of the distance between two points
Standard errors clustered at latitude-longitude degree grids - For example, a 2 by 2 grid consisting of sixteen adjacent points.

Figure 24: Heat Map of the Probability of Conflict by Land Quality

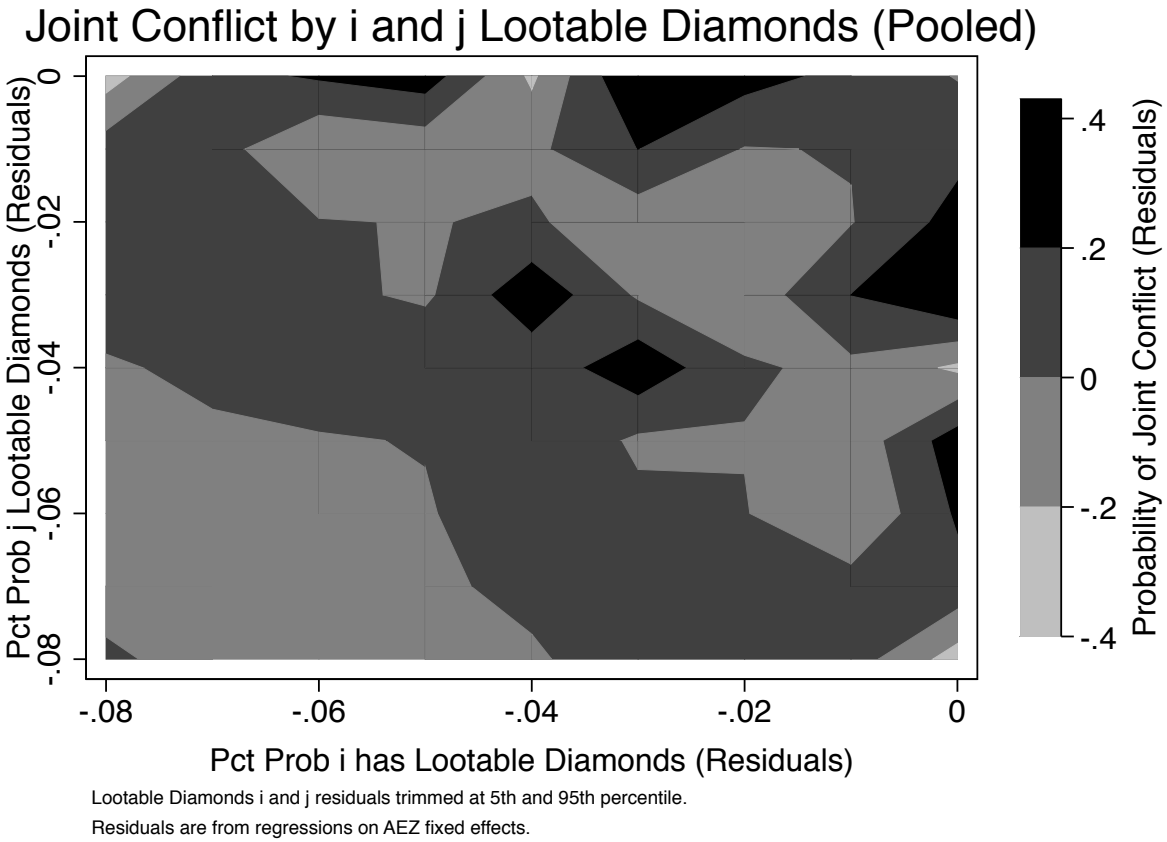

would not conform to the predictions of the model. Indeed, we find that the patterns are quite distinct than those predicted by the model. The heat map figure and table corresponding to the analysis using nonlootable diamonds are presented in the appendix.

5.3 Development (Night Time Illumination)

Finally, we present evidence of the relationship between development in point *i* as proxied by measures of night time illumination (lights) and rainfall in points *i* and j, net of any conflict, as predicted by the model in section 2. Figure 25 repeats the exercise in Figure 10 for lights as a function of rainfall in both points *i* and *j*. We see that the regions of joint conflict prevalence (e.g., upper-right) in Figure 10 correspond to low levels of lights or development; while the region of little to no conflict (i.e., lower-left) corresponds to moderate development as rainfall is low, but conflict is also low. These results are broadly

consistent with the predictions of the model.

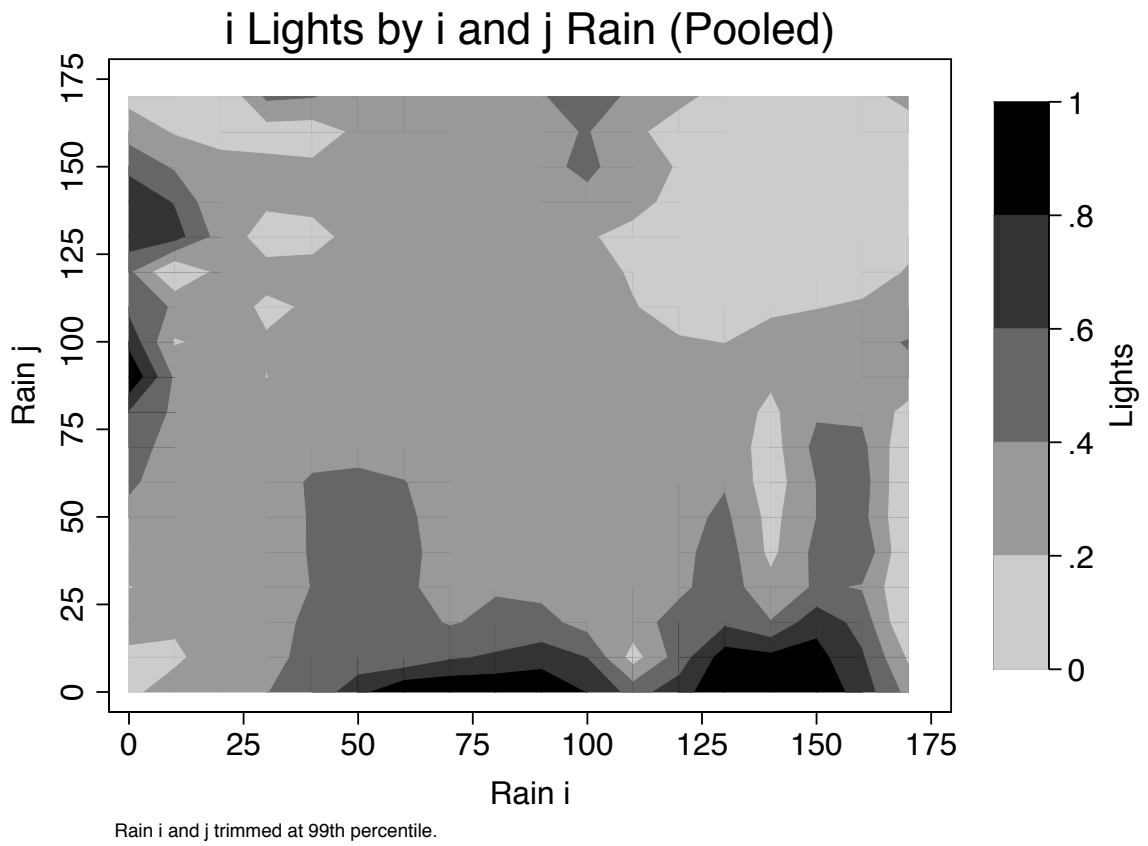

Figure 25: Heat Map of Light-Density by Long-Run Rainfall

In Table 8 we show how light-density falls as rainfall crosses the estimated cutoffs. Using the cutoffs estimated for the conflict regression, we regress light-density on the cutoffs, controlling for continuous measures of rainfall. Consistent with the other results in the paper and the predictions of the model, we show that light density falls at each of these cutoffs, showing how an increase in conflict may lead to a fall in local economic activity. Lastly, we conduct the analogous regression discontinuity analysis for light-density at the previously estimated rainfall cutoffs. The results from these analyses are presented in the appendix and once again lend further support to the predictions of the model.

Table 8: Effect on Light Density

	Light Density			
$\mathbb{1}(rain_i > rain^{cutoff})$	-0.391	-0.124	-0.117	-0.0556
	(0.0770)***	(0.0591)**	(0.0587)**	(0.0507)
$\mathbb{1}(rain_j > rain^{cutoff})$	-0.0707	-0.112	-0.128	-0.0173
	(0.0386)*	(0.0257)***	(0.0280)***	(0.0137)
$\mathbb{1}(rain_i \& rain_j > rain^{cutoff})$	-0.120	-0.706	-1.066	-0.925
	(0.241)	(0.223)***	(0.244)***	(0.239)***
R-squared	0.007	0.436	0.450	0.509
Fixed Effects	None	None	AEZ	Grid 7
Controls	None	All	All	All
Observations		802,553		
Estimated rain cutoff		88.667		

Notes: Regressions of light density in 2008 on rainfall for the region and neighboring region being above an estimated cutoff.
Search algorithm for rainfall cutoffs described in the empirical section and estimated cutoff is reported in the table above. One-third of the sample (1604623 observations) were randomly selected for the search procedure.
Observations including region i&j pairs where region j is within 500 kilometers of region i-data is averaged over a ten year period between 1998 and 2008.
Controls include (for both points i and j) continuous measures of rainfall, latitude, longitude, ruggedness index, land quality index, humidity, malaria, population density, and a quadratic of the distance between two points
Standard errors clustered at 0.5 by 0.5 latitude-longitude degree grids.

6 Conclusion

We have presented an economic model of conflict in which two groups struggle over the division of resources. We consider a case in which a greater natural endowment raises a society's fighting capacity but also increases the returns gained by its neighbors in the event of a successful raid. Our model predicts outcomes that reflect these incentives: a greater own endowment and a greater neighbor's endowment both predict a greater likelihood of conflict. That is, we argue that there exists a 'rapacity effect' that motivates conflict. Further, the empowerment effect of greater own resources in our model outweighs the pacifying effects of a greater opportunity cost of conflict. Extending this model to allow for the possibility of non-violent sharing of resources as might occur between members of the same ethnic group, we find that sharing attenuates both the rapacity and empowerment effects of resource endowments on conflicts.

We have tested this model using spatial data on the incidence of conflict across the whole of Africa. Over the past two decades, regions that have received more favorable medium-term endowments of rainfall have been more likely to engage in conflict, particularly when their neighbors have received similar favorable endowments. Although our focus has been on rainfall, other measures of resource accumulation, such as land quality, reveal similar patterns. As in our model, these effects are strongest when externalities are measured across ethnic boundaries. Our results are robust to several additional controls and to restricting identification to comparisons of locations within narrow geographic bands.

There are, of course, limitations to our analysis. Most of these are imposed by data availability. We have focused on an African sample due largely to the coincidence of spatial data on ethnicity, conflict, rainfall, and night-time lights covering a long period of time. Similarly, data availability restricts our analysis to recent decades. The generalizability of our work to other contexts or time periods will by necessity be left to later research. Similarly, the data that would permit us to disaggregate conflicts by type or motivation lack the spatial detail needed for our empirical work. Our focus on rainfall as a measure of resource accumulation is driven by our ability to measure it in a consistent format across a broad region where it is relevant to economic output.

Conflict matters for both economic growth and individual outcomes (Blattman and Miguel, 2010). We have advanced the existing literature by showing that the determinants of conflict operate at a fine spatial level, within countries and within narrow geo-

graphic regions. While the existing literature has focused narrowly on minerals and other point resources in considering the spatial dynamics of conflict (Caselli et al, forthcoming), we have noted that endowments such as land quality and rainfall that are present more broadly can also shape the locations of conflict. To our knowledge, we have presented the first empirical results showing that the impact of resources on conflict is heterogeneous across ethnic divides. We consider externalities and complementarities to a greater degree than previous work.

Our results are relevant for policymakers interested in anticipating the locations of future conflicts. Our results suggest that the existing literature has overemphasized the degree to which resource accumulation reduces conflict by increasing its opportunity cost, neglecting the empowerment effect of having more resources to employ in violence. This is particularly important in regions with strong ethnic divisions. As the impacts of climate change will fall unequally across African regions, (Kurukulasuriya et al, 2011) our results imply similar heterogeneity in the impact of these changes on the locations of African violence.

References

Abadie, A. and Gardeazabal, J. (2003). The Economic Costs of Conflict: A Case Study of the Basque Country. *American Economic Review*, 93(1):113–132.

Acemoglu, D., Johnson, S., and Robinson, J. A. (2001). The Colonial Origins of Comparative Development: An Empirical Investigation. *The American Economic Review*, 91(5):1369–1401.

Acemoglu, D. and Robinson, J. A. (2001). A theory of political transitions. *American Economic Review*, pages 938–963.

Alexeev, M. and Conrad, R. (2009). The elusive curse of oil. *The Review of Economics and Statistics*, 91(3):586–598.

Alsan, M. et al. (2013). The effect of the tsetse fly on African development. *Unpublished manuscript*.

Angrist, J. D., Imbens, G. W., and Krueger, A. B. (1999). Jackknife instrumental variables estimation. *Journal of Applied Econometrics*.

Angrist, J. D. and Krueger, A. B. (1995). Split-Sample Instrumental Variables Estimates of the Return to Schooling. *Journal of Business & Economic Statistics*.

Arbatli, C. E., Ashraf, Q. H., and Galor, O. (2015). The nature of conflict.

Bai, J. (1997a). Estimating Multiple Breaks One at a Time. *Econometric Theory*.

Bai, J. (1997b). Estimation of a Change Point in Multiple Regression Models. *Review of Economics and Statistics*.

Bai, J. (2010). Common breaks in means and variances for panel data. *Journal of Econometrics*.

Bai, J. and Perron, P. (1998). Estimating and testing linear models with multiple structural changes. *Econometrica*.

Bannon, I. and Collier, P. (2003). *Natural resources and violent conflict: options and actions*. World Bank publications.

Barrios, S., Bertinelli, L., and Strobl, E. (2010). Trends in rainfall and economic growth in Africa: A neglected cause of the African growth tragedy. *The Review of Economics and Statistics*, 92(2):350–366.

Bazzi, S. and Blattman, C. (2014). Economic Shocks and Conflict: The Evidence from Commodity Prices. *American Economic Journal: Macroeconomics 6(4)*.

Berman, N. and Couttenier, M. (2014). External shocks, internal shots: The geography of civil conflicts. *Forthcoming in the Review of Economics and Statistics*.

Berman, N., Couttenier, M., Rohner, D., and Thoenig, M. (2014). This mine is mine! How minerals fuel conflicts in Africa. *CEPR Discussion Paper No. DP10089*.

Besley, T. and Persson, T. (2010). State capacity, conflict, and development. *Econometrica*, 78(1):1–34.

Besley, T. and Persson, T. (2011). The logic of political violence. *The quarterly journal of economics*, page qjr025.

Blattman, C. and Miguel, E. (2010). Civil war. *Journal of Economic Literature*, 48(1):3–57.

Brückner, M. (2010). Population Size and Civil Conflict Risk: Is there a Causal Link?*. *The Economic Journal*, 120(544):535–550.

Brückner, M. and Ciccone, A. (2010). International Commodity Prices, Growth and the Outbreak of Civil War in Sub-Saharan Africa. *The Economic Journal*, 120(544):519–534.

Calonico, S., Cattaneo, M. D., and Titiunik, R. (2014). Robust Nonparametric Confidence Intervals for Regression-Discontinuity Designs. *Econometrica*.

Card, D., Mas, A., and Rothstein, J. (2008). Tipping and the Dynamics of Segregation. *Quarterly Journal of Economics*.

Caselli, F., Morelli, M., and Rohner, D. (2013). The geography of inter-state resource wars. Technical report, National Bureau of Economic Research.

Caselli, F. and Tesei, A. (2011). Resource windfalls, political regimes, and political stability. Technical report, Forthcoming in the Review of Economics and Statistics.

Dell, M., Jones, B. F., and Olken, B. A. (2012). Temperature shocks and economic growth: Evidence from the last half century. *American Economic Journal: Macroeconomics*, 4(3):66–95.

Dube, O. and Vargas, J. F. (2013). Commodity price shocks and civil conflict: Evidence from Colombia. *The Review of Economic Studies*, 80(4):1384–1421.

Esteban, J. M., Morelli, M., and Rohner, D. (2010). Strategic mass killings. *Institute for Empirical Research in Economics, University of Zurich Working Paper*, (486).

Fearon, J. D. (2005). Primary commodity exports and civil war. *Journal of conflict Resolution*, 49(4):483–507.

Gleditsch, N., Wallensteen, P., Eriksson, M., Sollenberg, M., and Strand, H. (2002). Armed conflict 1946-2001: A new dataset. *Journal of Peace Research*, 39(5):615–637.

Glick, R. and Taylor, A. (2009). Collateral Damage: Trade Disruption and the Economic Impact of War. *The Review of Economics and Statistics*, 92(1):102–127.

Gonzalo, J. and Pitarakis, J.-Y. (2002). Estimation and model selection based inference in single and multiple threshold models. *Journal of Econometrics*.

Gonzalo, J. and Wolf, M. (2005). Subsampling inference in threshold autoregressive models. *Journal of Econometrics*.

Grossman, H. I. (1991). A General Equilibrium Model of Insurrections. *The American Economic Review 81(4): 912-21.*

Grossman, H. I. and Kim, M. (1995). Swords or plowshares? A theory of the security of claims to property. *Journal of Political Economy*, pages 1275–1288.

Hallberg, J. D. (2012). PRIO conflict site 1989–2008: a geo-referenced dataset on armed conflict. *Conflict Management and Peace Science*, 29(2):219–232.

Hansen, B. E. (2000). Sample Splitting and Threshold Estimation. *Econometrica*.

Henderson, J. V., Storeygard, A., and Weil, D. N. (2012). Measuring economic growth from outer space. *American Economic Review*, 102(2):994–1028.

Hirshleifer, J. (1989). Conflict and rent-seeking functions: Ratio versus difference models of relative success. *Public Choice, 63, 101-12.*

Hsiang, S. M., Burke, M., and Miguel, E. (2013). Quantifying the influence of climate on human conflict. *Science*, 341(6151):1235367.

Jerven, M. (2013). *Poor numbers: how we are misled by African development statistics and what to do about it*. Cornell University Press.

Jia, R. (2014). Weather shocks, sweet potatoes and peasant revolts in historical China. *The Economic Journal*, 124(575):92–118.

Matsuura, K. and Willmott, C. J. (2009). Terrestrial precipitation: 1900–2008 gridded monthly time series. *Center for Climatic Research Department of Geography Center for Climatic Research, University of Delaware*.

Mehlum, H., Moene, K., and Torvik, R. (2006). Institutions and the resource curse*. *The economic journal*, 116(508):1–20.

Michalopoulos, S. and Papaioannou, E. (2011). The Long-Run Effects of the Scramble for Africa. *NBER Working Paper No. 17620*.

Michalopoulos, S. and Papaioannou, E. (2013). Pre-Colonial Ethnic Institutions and Contemporary African Development. *Econometrica*, 81(1):113–152.

Miguel, E. and Satyanath, S. (2011). Re-examining Economic Shocks and Civil Conflict. *American Economic Journal: Applied Economics, 3(4): 228-232.*

Mitra, A. and Ray, D. (2013). Implications of an Economic Theory of Conflict: Hindu-Muslim Violence in India. *Journal of Political Economy 122, 719-765, 2014*.

Murdock, G. P. (1959). *Africa: its peoples and their culture history*. McGraw-Hill New York.

Nunn, N. and Puga, D. (2012). Ruggedness: The blessing of bad geography in Africa. *Review of Economics and Statistics*, 94(1):20–36.

Nunn, N. and Qian, N. (2014). Us food aid and civil conflict. *The American Economic Review*, 104(6):1630–1666.

Nunn, N. and Wantchekon, L. (2011). The Slave Trade and the Origins of Mistrust in Africa. *The American Economic Review*, 101(7):3221–3252.

Politis, D. N. and Romano, J. P. (1994). Large Sample Confidence Regions Based on Subsamples under Minimal Assumptions. *The Annals of Statistics*.

Raleigh, C., Cunningham, D., Wilhelmsen, L., and Gleditsch, N. P. (2006). Conflict Sites 1946–2005. *UCDP/PRIO Armed Conflicts Dataset Codebook. PRIO: Centre for the study of civil war. Version*, 2.

Rohner, D., Thoenig, M., and Zilibotti, F. (2013). Seeds of distrust: Conflict in Uganda. *Forthcoming, Journal of Economic Growth*, 18(3):217–252.

Sachs, J. D. and Warner, A. M. (1995). Natural resource abundance and economic growth. Technical report, National Bureau of Economic Research.

Skaperdas, S. (1992). Cooperation, Conflict, and Power in the Absence of Property Rights. *American Economic Review, 82(4): 720-39.*

A Nash Equilibria Proofs

A.1 Baseline Model

Lemma A.1 *For $r_i, r_j \in (0, \frac{c}{\delta})$, (N, N) is the unique pure-strategy Nash Equilibrium.*

Proof. Consider i's best response to $s_j = N$. i will choose N iff $r_i > r_i - c + \delta r_j$, which reduces to $\frac{c}{\delta} > r_j$. Similarly, j's best response to $s_i = N$ is N iff $\frac{c}{\delta} > r_i$. Thus for $r_i, r_j \in (0, \frac{c}{\delta})$, N constitutes the best response to N for both i and j, and we have that (N, N) is a Nash equilibrium.

To show that (N, N) is the unique NE in this case, it must be that (R, R) *is not* an NE.[8] We can show that (R, R) will not lie in this region. Take i's best response to $s_j = R$. This best response is R iff

$$(1-\delta)r_i < p(r_i - c + \delta(r_j - c)) + (1-p)(1-\delta)(r_i - c). \tag{6}$$

Given $p = \frac{r_i}{r_i + r_j}$, this inequality is equivalent to

$$r_j < \frac{-\delta r_k^2 + c(1+\delta)r_k}{\delta r_k - c(1-\delta)} \quad \text{for} \quad r_i \in (0, c\frac{1-\delta}{\delta}) \tag{7}$$

$$r_j > \frac{-\delta r_k^2 + c(1+\delta)r_k}{\delta r_k - c(1-\delta)} \quad \text{for} \quad r_i \in (c\frac{1-\delta}{\delta}, \frac{c}{\delta}) \tag{8}$$

Equation 7 would require that $r_j < 0$ and equation 8 that $r_j > \frac{c}{\delta}$. There is thus no $r_i, r_j \in (0, \frac{c}{\delta})$ for which the R is the best response for $s_j = R$

■

Lemma A.2 *Let $\psi(r_k) := \frac{-\delta r_k^2 + c(1+\delta)r_k}{\delta r_k - c(1-\delta)}$. (R, R) is the unique pure strategies Nash Equilibrium in the region $\{(r_i, r_j) : r_i \in (c\frac{1-\delta}{\delta}, \infty), r_j > \psi(r_i)\} \cap \{(r_i, r_j) : r_j \in (c\frac{1-\delta}{\delta}, \infty), r_i > \psi(r_j)\}$*

Proof. Consider i's best response to $s_j = R$ in this region. i will choose R iff $p(r_i - c + \delta(r_j - c)) + (1-p)(1-\delta)(r_i - c) > (1-\delta)r_i$, which amounts to the region $\{(r_i, r_j) : r_i \in$

[8] Note that for $r_i, r_j \in (0, \frac{c}{\delta})$, (R, N) and (N, R) cannot be NE, given that if one party plays N, the other's best response must be N for values of r_i and r_j in the specified range.

$(c\frac{1-\delta}{\delta}, \infty), r_j > \psi(r_i)\}$. Similarly j's best response to $s_i = R$ is R iff $(1-p)(r_j - c + \delta(r_i - c)) + p(1-\delta)(r_j - c) > (1-\delta)r_j$, which is the region $\{(r_i, r_j) : r_j \in (c\frac{1-\delta}{\delta}, \infty), r_i > \psi(r_j)\}$. Thus (R, R) is a Nash equilibrium in the intersection of these regions.

To show that (R, R) is the unique pure strategies Nash Equilibrium, it must be that (N, N) is not an equilibrium.[9] We can show that (N, N) cannot be an equilibrium in this region. i's best response to $s_j = N$ will be N iff $r_j < \frac{c}{\delta}$ and j's best response to $s_i = N$ will be N iff $r_i < \frac{c}{\delta}$. However, the intersections of the regions $\{(r_i, r_j) : r_i \in (c\frac{1-\delta}{\delta}, \infty), r_j > \psi(r_i)\} \cap \{(r_i, r_j) : r_j \in (c\frac{1-\delta}{\delta}, \infty), r_i > \psi(r_j)\}$ and the region $r_i, r_j \in (0, \frac{c}{\delta})$ is a null set. In $\mathbb{R}^2_+$, $\psi(r_i) = \psi(r_k)$ at the point $(\frac{c}{\delta}, \frac{c}{\delta})$. There is therefore no region in $\mathbb{R}^2_+$, for which $r_i > \psi(r_j), r_j > \psi(r_i)$ and $r_i, r_j \in (0, \frac{c}{\delta})$.

■

Lemma A.3 *Let* $\psi(r_k) := \frac{-\delta r_k^2 + c(1+\delta)r_k}{\delta r_k - c(1-\delta)}$. (N, R) *is the unique pure strategies Nash Equilibrium in the region* $\{(r_i, r_j) : r_i \in (\frac{c}{\delta}, \infty), r_j < \psi(r_i)\}$

Proof. Consider i's best response to $s_j = R$ in this region. i will choose N iff $p(r_i - c + \delta(r_j - c)) + (1-p)(1-\delta)(r_i - c) < (1-\delta)r_i$, which amounts to the region $\{(r_i, r_j) : r_i \in (c\frac{1-\delta}{\delta}, \infty), r_j < \psi(r_i)\}$. Similarly j's best response to $s_i = N$ is R iff $\frac{c}{\delta} < r_i$. Thus (N, R) is a Nash equilibrium if $r_i > \frac{c}{\delta}$ and $r_j < \psi(r_i)$.

To show that (N, R) is the unique pure strategies Nash Equilibrium, we must rule out the other equilibria. (N, N) can be ruled out because j's best response $s_i = N$ cannot be N if $\frac{c}{\delta} < r_i$. Similarly, (R, R) cannot be a Nash Equilibrium in this region because i's best response to $s_j = R$ cannot be R if $\{(r_i, r_j) : r_i \in (\frac{c}{\delta}, \infty), r_j < \psi(r_i)\}$. Lastly, we must rule out (R, N). i's best response to $s_j = N$ is R iff $r_j > \frac{c}{\delta}$. However, $\{(r_i, r_j) : r_i \in (\frac{c}{\delta}, \infty), r_j < \psi(r_i)\} \cap \{(r_i, r_j) : r_j > \frac{c}{\delta}\} = \emptyset$, thus precluding an (R, N) equilibrium in this region.

■

Lemma A.4 *Let* $\psi(r_k) := \frac{-\delta r_k^2 + c(1+\delta)r_k}{\delta r_k - c(1-\delta)}$. (R, N) *is the unique pure strategies Nash Equilibrium in the region* $\{(r_i, r_j) : r_j \in (\frac{c}{\delta}, \infty), r_i < \psi(r_j)\}$

Proof. Consider j's best response to $s_i = R$ in this region. j will choose N iff $\{(r_i, r_j) : r_j \in (c\frac{1-\delta}{\delta}, \infty), r_i < \psi(r_j)\}$. Similarly i's best response to $s_j = N$ is R iff $\frac{c}{\delta} < r_j$. Thus (R, N) is a Nash equilibrium if $r_j > \frac{c}{\delta}$ and $r_i < \psi(r_j)$.

[9] Note that in this region, (R, N) and (N, R) cannot be NE, given that if one party plays R, the other's best response must be R for values of r_i and r_j in the specified range.

To show that (R, N) is the unique pure strategies Nash Equilibrium, we must rule out the other equilibria. (N, N) can be ruled out because i's best response $s_j = N$ cannot be N if $\frac{c}{\delta} < r_j$. Similarly, (R, R) cannot be a Nash Equilibrium in this region because j's best response to $s_i = R$ cannot be R if $\{(r_i, r_j) : r_j \in (\frac{c}{\delta}, \infty), r_i < \psi(r_j)\}$. Lastly, we must rule out (N, R). j's best response to $s_i = N$ is R iff $r_i > \frac{c}{\delta}$. However, $\{(r_i, r_j) : r_j \in (\frac{c}{\delta}, \infty), r_i < \psi(r_j)\} \cap \{(r_i, r_j) : r_i > \frac{c}{\delta}\} = \emptyset$, thus preventing the possibility of an (N, R) equilibrium in this region.

■

A.2 Sharing Rule

Lemma A.5 *Let $\chi(r_k) = \frac{c - \phi r_k}{\delta - \phi}$. (N, N) is the unique pure-strategy Nash Equilibrium for the region $\{(r_i, r_j) : r_j < \chi(r_i),\ r_i < \chi(r_j)\}$.*

Proof. Consider i's best response to $s_j = N$. i will choose N iff $(1 - \phi)r_i + \phi r_j > r_i - c + \delta r_j$, which reduces to $\chi(r_i) > r_j$. Similarly, j's best response to $s_i = N$ is N iff $\chi(r_i) > r_i$. Thus for $\{(r_i, r_j) : r_j < \chi(r_i),\ r_i < \chi(r_j)\}$, N constitutes the best response to N for both i and j, and we have that (N, N) is a Nash equilibrium.

To show that (N, N) is the unique NE in this case, it must be that (R, R) *is not* an NE.[10] We can show that (R, R) will not lie in this region. Take i's best response to $s_j = R$. This best response is R iff

$$(1 - \delta)r_i < p(r_i - c + \delta(r_j - c)) + (1 - p)(1 - \delta)(r_i - c). \tag{9}$$

Given $p = \frac{r_i}{r_i + r_j}$, this inequality is equivalent to

$$r_j < \frac{-\delta r_k^2 + c(1 + \delta)r_k}{\delta r_k - c(1 - \delta)} \quad \text{for} \quad r_i \in (0, c\frac{1 - \delta}{\delta}) \tag{10}$$

$$r_j > \frac{-\delta r_k^2 + c(1 + \delta)r_k}{\delta r_k - c(1 - \delta)} \quad \text{for} \quad r_i \in (c\frac{1 - \delta}{\delta}, \frac{c}{\phi}) \tag{11}$$

Equation 10 would require that $r_j < 0$ and equation 11 that $r_j > \chi(r_i)$ for $\delta > \phi > \frac{\delta}{1 + \delta}$.

[10] Note that for $r_i, r_j \in (0, \frac{c}{\delta})$, (R, N) and (N, R) cannot be NE, given that if one party plays N, the other's best response must be N for values of r_i and r_j in the specified range.

There is thus no $\{(r_i, r_j) : r_j < \chi(r_i),\ r_i < \chi(r_j)\}$ for which the R is the best response for $s_j = R$

■

Lemma A.6 *Let* $\psi(r_k) := \frac{-\delta r_k^2 + c(1+\delta)r_k}{\delta r_k - c(1-\delta)}$. (R, R) *is the unique pure strategies Nash Equilibrium in the region* $\{(r_i, r_j) : r_i \in (c\frac{1-\delta}{\delta}, \infty), r_j > \psi(r_i)\} \cap \{(r_i, r_j) : r_j \in (c\frac{1-\delta}{\delta}, \infty), r_i > \psi(r_j)\}$

Proof. Consider i's best response to $s_j = R$ in this region. i will choose R iff $p(r_i - c + \delta(r_j - c)) + (1-p)(1-\delta)(r_i - c) > (1-\delta)r_i$, which amounts to the region $\{(r_i, r_j) : r_i \in (c\frac{1-\delta}{\delta}, \infty), r_j > \psi(r_i)\}$. Similarly j's best response to $s_i = R$ is R iff $(1-p)(r_j - c + \delta(r_i - c)) + p(1-\delta)(r_j - c) > (1-\delta)r_j$, which is the region $\{(r_i, r_j) : r_j \in (c\frac{1-\delta}{\delta}, \infty), r_i > \psi(r_j)\}$. Thus (R, R) is a Nash equilibrium in the intersection of these regions.

To show that (R, R) is the unique pure strategies Nash Equilibrium, it must be that (N, N) is not an equilibrium.[11] We can show that (N, N) cannot be an equilibrium in this region. i's best response to $s_j = N$ will be N iff $r_j < \frac{c}{\delta}$ and j's best response to $s_i = N$ will be N iff $r_i < \frac{c}{\delta}$. However, the intersections of the regions $\{(r_i, r_j) : r_i \in (c\frac{1-\delta}{\delta}, \infty), r_j > \psi(r_i)\} \cap \{(r_i, r_j) : r_j \in (c\frac{1-\delta}{\delta}, \infty), r_i > \psi(r_j)\}$ and the region $r_i, r_j \in (0, \frac{c}{\delta})$ is a null set. In $\mathbb{R}^2_+$, $\psi(r_i) = \psi(r_k)$ at the point $(\frac{c}{\delta}, \frac{c}{\delta})$. There is therefore no region in $\mathbb{R}^2_+$, for which $r_i > \psi(r_j), r_j > \psi(r_i)$ and $r_i, r_j \in (0, \frac{c}{\delta})$.

■

Lemma A.7 *Let* $\psi(r_k) := \frac{-\delta r_k^2 + c(1+\delta)r_k}{\delta r_k - c(1-\delta)}$, *and let* $\chi(r_k) = \frac{c - \phi r_k}{\delta - \phi}$. (N, R) *is the unique pure strategies Nash Equilibrium in the region* $\{(r_i, r_j) : r_i \in (0, \frac{c}{\delta} - c), \chi(r_j) < r_i\} \cup \{(r_i, r_j) : r_i \in (\frac{c}{\delta} - c, \infty), r_j < \psi(r_i)\}$

Proof. Consider i's best response to $s_j = R$ in this region. i will choose N iff $p(r_i - c + \delta(r_j - c)) + (1-p)(1-\delta)(r_i - c) < (1-\delta)r_i$, which amounts to the region $\{(r_i, r_j) : r_i \in (c\frac{1-\delta}{\delta}, \infty), r_j < \psi(r_i)\}$. Similarly j's best response to $s_i = N$ is R iff $\chi(r_j) < r_i$. Thus (N, R) is a Nash equilibrium in the region $\{(r_i, r_j) : r_i \in (0, \frac{c}{\delta} - c), \chi(r_j) < r_i\} \cup \{(r_i, r_j) : r_i \in (\frac{c}{\delta} - c, \infty), r_j < \psi(r_i)\}$.

To show that (N, R) is the unique pure strategies Nash Equilibrium, we must rule out the other equilibria. (N, N) can be ruled out because j's best response $s_i = N$ cannot be

[11] Note that in this region, (R, N) and (N, R) cannot be NE, given that if one party plays R, the other's best response must be R for values of r_i and r_j in the specified range.

N if $\chi(r_j) < r_i$. Similarly, (R, R) cannot be a Nash Equilibrium in this region because i's best response to $s_j = R$ cannot be R if $\{(r_i, r_j) : r_i \in (\frac{c}{\delta}, \infty), r_j < \psi(r_i)\}$. Lastly, we must rule out (R, N). i's best response to $s_j = N$ is R iff $r_j > \chi(r_i)$. However, $\{(r_i, r_j) : r_i \in (\frac{c}{\delta}, \infty), r_j < \psi(r_i)\} \cap \{(r_i, r_j) : r_j > \chi(r_i)\} = \emptyset$, thus precluding an (R, N) equilibrium in this region.

■

Lemma A.8 *Let* $\psi(r_k) := \frac{-\delta r_k^2 + c(1+\delta) r_k}{\delta r_k - c(1-\delta)}$, *and let* $\chi(r_k) = \frac{c - \phi r_k}{\delta - \phi}$. (R, N) *is the unique pure strategies Nash Equilibrium in the region* $\{(r_i, r_j) : r_j \in (0, \frac{c}{\delta} - c), \chi(r_i) < r_j\} \cup \{(r_i, r_j) : r_j \in (\frac{c}{\delta} - c, \infty), r_i < \psi(r_j)\}$

Proof. Consider j's best response to $s_i = R$ in this region. j will choose N iff $\{(r_i, r_j) : r_j \in (c\frac{1-\delta}{\delta}, \infty), r_i < \psi(r_j)\}$. Similarly i's best response to $s_j = N$ is R iff $\chi(r_i) < r_j$. Thus (R, N) is a Nash equilibrium in the region $\{(r_i, r_j) : r_j \in (0, \frac{c}{\delta} - c), \chi(r_i) < r_j\} \cup \{(r_i, r_j) : r_j \in (\frac{c}{\delta} - c, \infty), r_i < \psi(r_j)\}$.

To show that (R, N) is the unique pure strategies Nash Equilibrium, we must rule out the other equilibria. (N, N) can be ruled out because i's best response $s_j = N$ cannot be N if $\chi(r_i) < r_j$. Similarly, (R, R) cannot be a Nash Equilibrium in this region because j's best response to $s_i = R$ cannot be R if $\{(r_i, r_j) : r_j \in (\frac{c}{\delta}, \infty), r_i < \psi(r_j)\}$. Lastly, we must rule out (N, R). j's best response to $s_i = N$ is R iff $r_i > \chi(r_j)$. However, $\{(r_i, r_j) : r_j \in (\frac{c}{\delta}, \infty), r_i < \psi(r_j)\} \cap \{(r_i, r_j) : r_i > \chi(r_j)\} = \emptyset$, thus precluding an (N, R) equilibrium in this region.

■

B Additional Tables and Figures

Figure 26: Distribution of Resources Across the African Continent

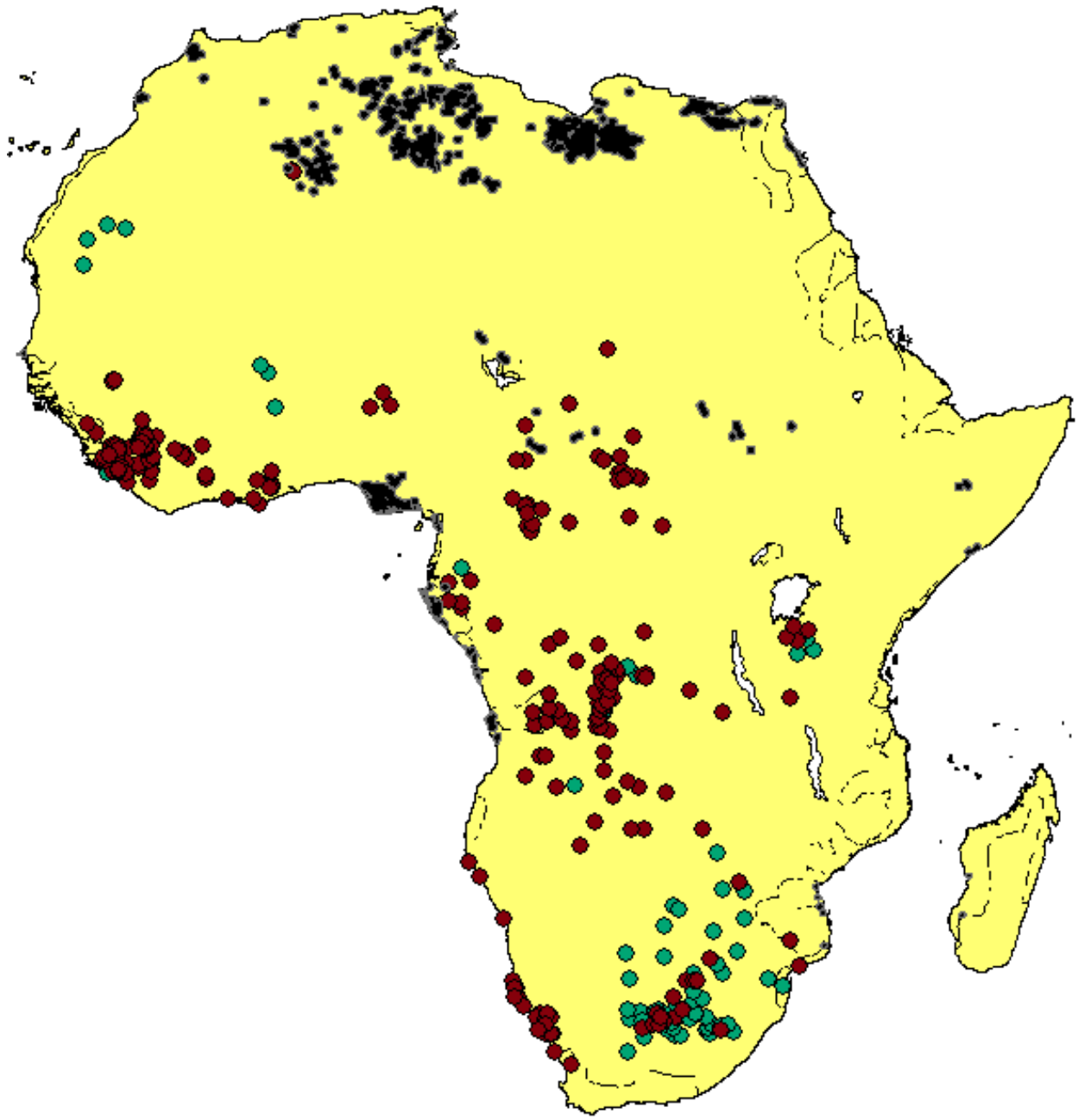

Legend: Black dots represent oil fields, red dots are lootable diamond mines and green dots are non-lootable diamond mines

Figure 27: Lights RD at the Rain i-cutoff

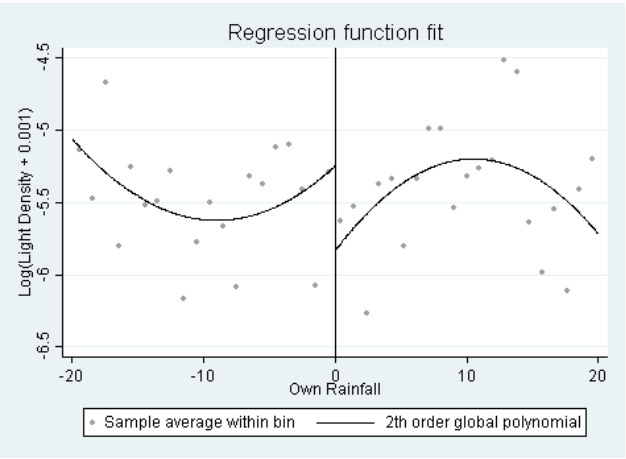

Figure 28: Lights RD at the Rain j-cutoff

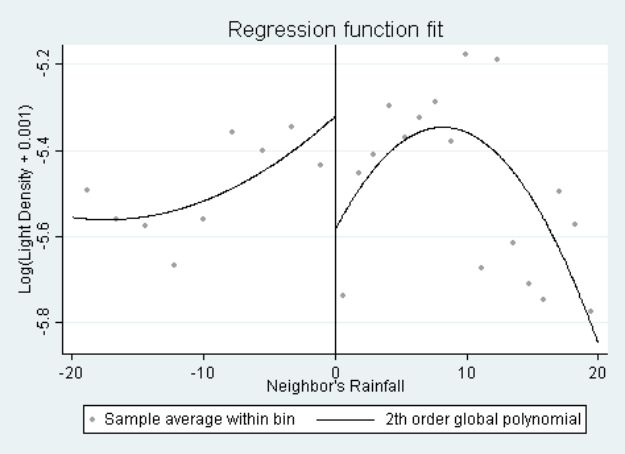

RD graphs of Log Light Density on rainfall. Graphs were produced using the Calonico, Cattaneo and Tituinik (2014) procedure of identifying the optimal bin sizes.

Figure 29: Lights RD at the Rain i-cutoff, Rain *j* below cutoff

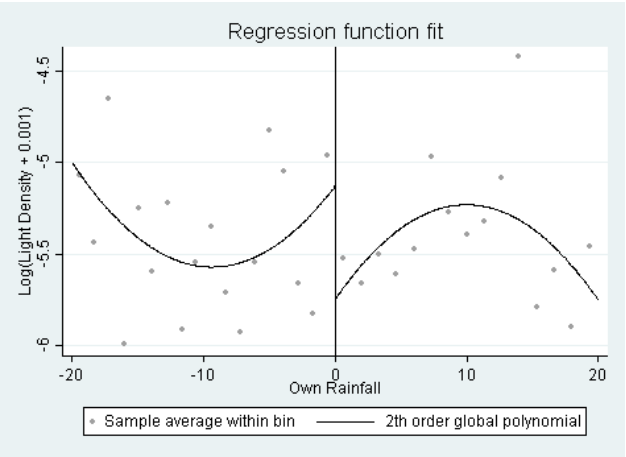

Figure 30: Lights RD at the Rain j-cutoff, Rain *i* below cutoff

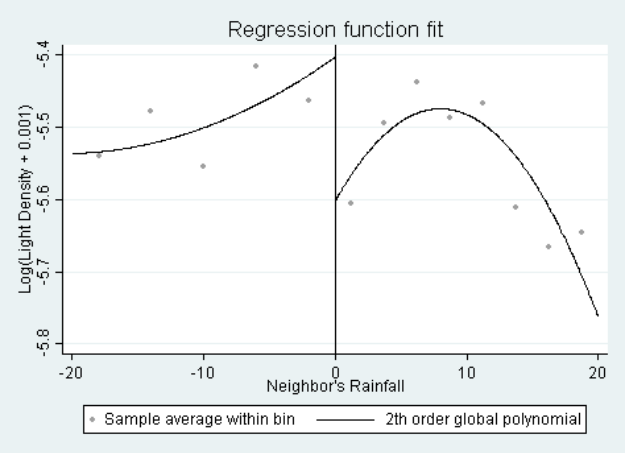

RD graphs of Log Light Density on rainfall. Graphs were produced using the Calonico, Cattaneo and Tituinik (2014) procedure of identifying the optimal bin sizes.

Figure 31: Lights RD at the Rain i-cutoff, Rain *j* above cutoff

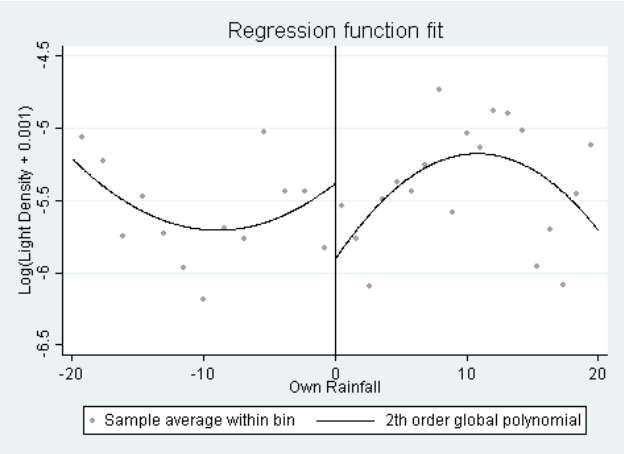

Figure 32: Lights RD at the Rain j-cutoff, Rain *i* above cutoff

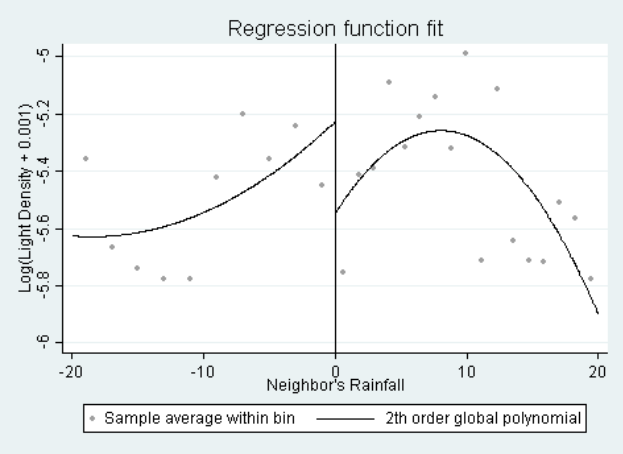

RD graphs of Log Light Density on rainfall. Graphs were produced using the Calonico, Cattaneo and Titunik (2014) procedure of identifying the optimal bin sizes.

Figure 33: Heat Map of the Probability of Conflict by Land Quality

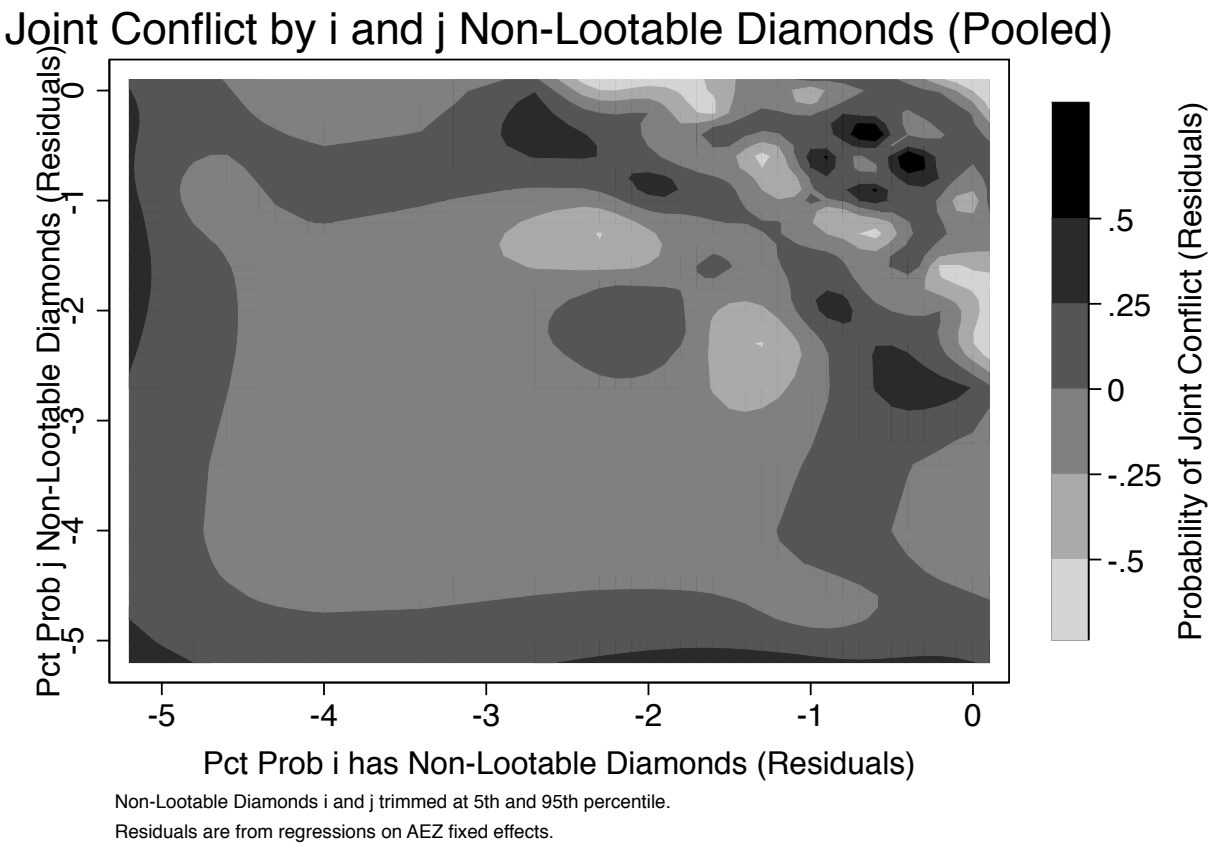

C Tables

Table 9: Conflict Intensity and Nonlootable Diamonds

Dependent Variable: Probability(Region i&j in same conflict between 1998-2008)				
Nonlootable Diamonds-i	-0.252	-0.0643	-0.0752	0.0368
SE cluster: Point *i*	(0.0376)***	(0.0279)**	(0.0234)***	(0.0113)***
2 by 2 grid	(0.0609)***	(0.0404)	(0.0347)**	(0.0214)*
2-way: Point i&j	(0.0383)***	(0.0284)**	(0.0340)**	(0.0459)
Nonlootable Diamonds-j	-0.252	-0.0643	-0.0496	0.0343
SE cluster: Point *i*	(0.00764)***	(0.00600)***	(0.00614)***	(0.00248)***
2 by 2 grid	(0.0278)***	(0.0216)***	(0.0201)**	(0.00723)***
2-way: Point i&j	(0.0383)***	(0.0284)**	(0.0327)	(0.0448)
Nonlootable Diamonds-i&j	0.132	0.0239	-0.0109	-0.0508
SE cluster: Point *i*	(0.0256)***	(0.0203)	(0.0169)	(0.00851)***
2 by 2 grid	(0.0492)***	(0.0312)	(0.0259)	(0.0154)***
2-way: Point i&j	(0.0354)***	(0.0282)	(0.0343)	(0.0464)
R-squared				
Fixed Effects	None	None	AEZ	Grid 7 by 7
Controls - point i	None	All	All	All
Controls - point j	None	All	All	All
Observations		802,553		
Mean dependent var		0.455		

Notes: Regressions of ever being involved in the same conflict over a ten year period (1998 to 2008) on whether or not the region has non lootable diamond mines.
Observations including region i&j pairs where region *j* is within 500 kilometers of region i- data is averaged over a ten year period between 1998 and 2008.
Controls include (for both points *i* and j) latitude, longitude, ruggedness index, land quality index, humidity, malaria, population density, and a quadratic of the distance between two points
Standard errors clustered at latitude-longitude degree grids - For example, a 2 by 2 grid consisting of sixteen adjacent points.